FLOW-DISTRIBUTED SPIKES FOR SCHNAKENBERG KINETICS

JUNCHENG WEI,
DEPARTMENT OF MATHEMATICS,
THE CHINESE UNIVERSITY OF HONG KONG,
SHATIN, HONG KONG
AND MATTHIAS WINTER,
BRUNEL UNIVERSITY, DEPARTMENT OF MATHEMATICAL SCIENCES,
UXBRIDGE, UB8 3PH,
UNITED KINGDOM
CORRESPONDING AUTHOR, EMAIL: MATTHIAS.WINTER@BRUNEL.AC.UK

ABSTRACT. We study a system of reaction-diffusion-convection equations which combine a reaction-diffusion system with Schnakenberg kinetics and the convective flow equations. It serves as a simple model for flow-distributed pattern formation. We show how the choice of boundary conditions and the size of the flow influence the positions of the emerging spiky patterns and give conditions when they are shifted to the right or to the left. Further, we analyze the shape and prove the stability of the spikes. The importance of these results for biological applications, in particular the formation of left-right asymmetry in the mouse, is indicated.

1. INTRODUCTION

A model for the development of handedness in left/right asymmetry has been suggested by Brown and Wolpert [2] which is based on three separate phenomena: (i) conversion from molecular handedness to handedness at the cellular level, (ii) random generation of asymmetry, e.g. by a reaction-diffusion process (iii) an interpretation process which leads to the development of different structures on the left and right. This model can explain many phenomena observed for various species e.g. for *situs inversus viscerum* mutation for *triturus* or in the mouse and bilateral asymmetry for sea urchins. Human diseases like the Ivemark syndrome or Kartegener's syndrome can be understood in this context as well. In particular, the model gives a good explanation why a loss of conversion of asymmetry from a molecular or some other local source does not result in symmetry but in random asymmetry.

Although they suggest a molecular basis for handedness, alternative approaches to left/right symmetry breaking include electric currents flowing in anterior to posterior direction [6] or fluid flow, e.g. nodal flow in the mouse, which might be initialized by rotation of monocilia and then sustained and driven by interaction with a reaction-diffusion mechanism, e.g. based on an interaction of the *Nodal* and *Lefty* proteins to establish the left/right asymmetry [5], [13].

Therefore it is interesting, on a theoretical level, to investigate the influence of a flow on reaction-diffusion system. In this paper we will consider the special case of flow-distributed spikes. We will pay particular attention to the way in which the fluid flow breaks the left/right symmetry in the system: Without convective flow the spike is located in the center of an interval. The flow will shift

1991 *Mathematics Subject Classification.* Primary 35B36, 92E20; Secondary 35B35, 76E06.
Key words and phrases. Pattern Formation, Convection, Spike, Steady-States, Stability, Left/Right Asymmetry.

it to the left or right half of the domain, depending on the boundary conditions and the size of the flow.

In particular, we study the effect of convective flow in a pattern-forming reaction-diffusion system. As a prototype, we consider Schnakenberg kinetics and combine it with the convective flow equations.

For both diffusion and convection processes the transport is driven by a flux which for diffusion is defined as the concentration gradient and for convection as the concentration gradient minus a constant times the concentration.

In a closed system the flux will vanish at the boundary which for a convective system leads to Robin boundary conditions (zero flux). For convective systems we will also consider Neumann boundary conditions (zero diffusive flux). We will see that changing the boundary conditions will result in strikingly different behavior of the system.

The pattern under consideration will be an interior single-spike pattern which will be studied for either type of boundary conditions. For Neumann boundary conditions the spike will be shifted either in the same direction as or in the opposite direction of the convective flow, depending on the size of the convection (Section 2). This result is summarized in Theorem 2.1.

In contrast, for Robin boundary conditions the spike will always be shifted in the same direction as the convective flow (Section 3). This result is given in Theorem 3.1.

Further, we will show analytically that the one-spike solution is always stable (Sections 4–6). This result is formulated in Theorem 6.1.

Our analytical results will be supported by numerical computations. We will present simulations showing that for Neumann boundary conditions the spike can be shifted in the same/opposite direction of the convective flow (Figures 1-2) and for Robin boundary conditions it will always be shifted in the same direction as the flow (Figure 3). Further, we will compute some examples of multiple spikes, both for Neumann boundary conditions (Figure 4) and Robin boundary conditions (Figures 5-6) which indicate that the spikes now have varying amplitudes and irregular spacing (Section 7). Multiple spikes are not analysed in this paper, but these issues are work in progress which we leave for future work. The importance of these mathematical results for biological application, in particular for the formation of left-right asymmetry in mouse is discussed (Section 8).

We call the spikes in this reaction-diffusion-convection system flow-distributed spikes (FDS) following the terminology of Satnoianu, Maini and Menzinger [16]. The influence of flow on pattern formation has been observed experimentally [8, 15]. Theoretical investigations have explained many features of this interaction [9, 11, 12, 16, 20, 21], in particular new instabilities and stabilization [10, 19, 22], boundary forcing [17], or phase differences [18] have been established and linked to the Turing instability. We show some qualitatively some of these features are also present for spikes.

The system to be investigated is given in the following form

$$\begin{cases} a_t = \delta a_{xx} - \delta\alpha a_x + \frac{1}{2} - cab^2, \\ b_t = b_{xx} - \alpha b_x - b + ab^2. \end{cases} \tag{1.1}$$

It can be derived as a prototype model for the interaction of an electric field and an ionic version of an autocatalytic system [11, 12, 17].

Rescaling the spatial variable $x = \frac{\overline{x}}{\epsilon}$ and setting $\delta = \frac{D}{\epsilon^2}$, $\alpha = \epsilon\overline{\alpha}$, we get

$$\begin{cases} a_t = Da_{\overline{x}\overline{x}} - D\overline{\alpha}a_{\overline{x}} + \frac{1}{2} - cab^2, \\ b_t = \epsilon^2 b_{\overline{x}\overline{x}} - \epsilon^2\overline{\alpha}b_{\overline{x}} - b + ab^2. \end{cases} \tag{1.2}$$

Setting

$$a = \epsilon\hat{a}, \quad b = \frac{\hat{b}}{\epsilon}, \quad D = \frac{\hat{D}}{\epsilon},$$

we get after dropping hats and bars

$$\begin{cases} \epsilon a_t = Da_{xx} - D\alpha a_x + \frac{1}{2} - \frac{c}{\epsilon}ab^2, \\ b_t = \epsilon^2 b_{xx} - \epsilon^2\alpha b_x - b + ab^2. \end{cases} \tag{1.3}$$

For a steady state this problem becomes

$$\begin{cases} 0 = Da_{xx} - D\alpha a_x + \frac{1}{2} - \frac{c}{\epsilon}ab^2, \\ 0 = \epsilon^2 b_{xx} - \epsilon^2\alpha b_x - b + ab^2. \end{cases} \tag{1.4}$$

Next we introduce suitable boundary conditions and consider single-spike steady-state solutions.

2. Neumann boundary conditions (zero diffusive flux)

First we investigate solutions of (1.4), i.e. steady-state solutions of (1.3), in the interval $\Omega = (-1, 1)$ with zero Neumann boundary conditions:

$$a_x = b_x = 0, \qquad \text{for } x = -1 \text{ or } x = 1. \tag{2.1}$$

These boundary conditions model zero diffusive flux.

Before stating our main results, let us introduce some notation. Let $L^2(-1, 1)$ and $H^2(-1, 1)$ be the usual Lebesgue and Sobolev spaces. Let w be the unique solution of the following problem:

$$\begin{cases} w_{yy} - w + w^2 = 0 \quad \text{in } \mathbb{R}^1, \\ w > 0, \\ w(0) = \max_{y\in\mathbb{R}} w(y), \\ w(y) \to 0 \quad \text{as } |y| \to \infty \end{cases} \tag{2.2}$$

In fact, it is easy to see that $w(y)$ can explicitly be written as

$$w(y) = \frac{3}{2}(\cosh y)^{-2}. \tag{2.3}$$

We use the norm

$$\|u\|_{H^2_\epsilon(-1,1)} = \|u\|_{H^2(\Omega_\epsilon)},$$

where $\Omega_\epsilon = \Omega/\epsilon = (-1/\epsilon, 1/\epsilon)$ and a similar notation is adapted for L^2 and H^1.

Theorem 2.1. *For ϵ small enough, there is a spiky solution (a_ϵ, b_ϵ) of the system (1.4) with Neumann boundary conditions (2.1). The shape of this solution is given by*

$$b_\epsilon(x) = \frac{1}{\xi_\epsilon} w\left(\frac{x - x_1^\epsilon}{\epsilon}\right) + O(\epsilon) \text{ in } H^2_\epsilon(-1, 1), \tag{2.4}$$

$$a_\epsilon(x_1^\epsilon) = \xi_\epsilon, \tag{2.5}$$

the amplitude satisfies

$$\xi_\epsilon = \xi_0 + O(\epsilon) \quad \textit{with} \quad \xi_0 = \frac{6c\alpha}{e^{\alpha x_1}\sinh\alpha} \tag{2.6}$$

and for the position we have

$$x_1^\epsilon = x_1^0 + O(\epsilon) \quad \textit{with} \quad x_1^0 = \frac{1}{\alpha}\ln\left(1+\sqrt{1+24Dc\alpha^3\coth\alpha}\right) - \frac{1}{\alpha}\ln(2\cosh\alpha). \tag{2.7}$$

Remarks:

1. Estimate (2.7) implies

$$x_1^\epsilon = \alpha\left(6Dc - \frac{1}{2}\right) + O(\alpha^2+\epsilon)$$

as α, $\epsilon \to 0$. Therefore, if $2\beta_0 Dc > 1$, then $x_1^\epsilon > 0$, and if $2\beta_0 Dc < 1$, then $x_1^\epsilon < 0$ for α, ϵ small enough; from (2.7) we also read off that $x_1^\epsilon < 0$ for α large enough and ϵ small enough.

2. Note that a is a slow function and b is a fast function with respect to the spatial variable x. Therefore, using their asymptotic behaviour, we have

$$\frac{c}{\epsilon}\int_{-1}^{1} ab^2\,dx = \frac{c}{\xi_\epsilon}\left(\int_{\mathbb{R}} w^2\,dy\right) + O(\epsilon) = \frac{e^{\alpha x_1}\sinh\alpha}{\alpha} + O(\epsilon). \tag{2.8}$$

Proof of Theorem 2.1:

We now construct a solution which concentrates near x_1^0.

For the rest of the paper, we assume that $x_1 \in B_{\epsilon^{3/4}}(x_1^0) = \{x \in \Omega : |x - x_1^0| < \epsilon^{3/4}\}$. Let $\chi : (-1,1) \to [0,1]$ be a smooth cut-off function such that

$$\chi(x) = 1 \text{ for } |x| < 1 \quad \text{and} \quad \chi(x) = 0 \text{ for } |x| > 2\delta. \tag{2.9}$$

Then we introduce the following approximate solution

$$b_{\epsilon,x_1}(x) = \frac{1}{\xi_\epsilon} w(y)\chi\left(\frac{x-x_1^0}{r_0}\right), \quad a_{\epsilon,x_1}(x) = T[b_{\epsilon,x_1}],$$

where $y = \epsilon^{-1}(x - x_1)$, $r_0 = \frac{1}{3}\min\{1 - x_1^0, 1 + x_1^0\}$ and $x_1 \in B_{\epsilon^{3/4}}(x_1^0)$ is to be determined. Here $T[A]$ for $A \in H^2(-1,1)$ is the unique solution of

$$DT[A]_{xx} - D\alpha T[A]_x + \frac{1}{2} - \epsilon^{-1}cT[A]A^2 = 0, \quad -1 < x < 1 \tag{2.10}$$

where $T[A]$ satisfies Neumann or Robin boundary conditions, respectively.

Multiplying (2.10) by $e^{-\alpha x}$ and integrating implies that $\xi_\epsilon = \xi_0 + O(\epsilon)$.

To determine the component a of the approximate solution, we use the representation formula given in (9.8) and get

$$a(x_0) = \frac{\alpha}{2\sinh\alpha}\int_{-1}^{1} e^{-\alpha x}a(x)\,dx + \frac{\alpha}{\sinh\alpha}\int_{-1}^{1} f(x)e^{-\alpha x}G(x,x_0)\,dx,$$

where

$$f(x) = \frac{c}{\epsilon}a(x)b^2(x) = \frac{c}{\epsilon\xi_\epsilon}w^2\chi^2 + O(\epsilon) \quad \text{in } H^2_\epsilon(-1,1)$$

and $G(x_0, x_1)$ is given by (9.10). Together with (2.8), this implies

$$a(x_0) = c_1 + \frac{\alpha}{\sinh\alpha}\frac{c}{\epsilon\xi_\epsilon}\int_{-1}^{1} w^2\left(\frac{x-x_1}{\epsilon}\right)e^{-\alpha x}G(x,x_0)\,dx + O(\epsilon)$$

$$= c_1 + \frac{\alpha}{\sinh\alpha}\frac{c}{\xi_\epsilon}e^{-\alpha x_1}G(x_1,x_0)\int_{\mathbb{R}} w^2\,dy + O(\epsilon) + O(\epsilon)$$

$$= c_1 + G(x_1,x_0) + O(\epsilon) \tag{2.11}$$

with the real constant

$$c_1 = \frac{\alpha}{2\sinh\alpha}\int_{-1}^{1} e^{-\alpha x}a(x)\,dx.$$

We are now going to compute the integral in the constant c_1.

Setting $x_1 = x_0$ in (2.11) and using (2.6), we get

$$\frac{\alpha}{\sinh\alpha}6ce^{-\alpha x_1} = \frac{\alpha}{2\sinh\alpha}\int_{-1}^{1} e^{-\alpha x}a(x)\,dx + G(x_1,x_1) + O(\epsilon). \tag{2.12}$$

Substituting (2.12) into (2.11) gives

$$a(x_0) = \frac{\alpha}{\sinh\alpha}6ce^{-\alpha x_1} - G(x_1,x_1) + G(x_1,x_0) + O(\epsilon)$$

$$= \frac{\alpha}{\sinh\alpha}6ce^{-\alpha x_1} - \frac{x_1}{D\alpha} + \frac{1}{D\alpha^2}e^{\alpha x_1}\cosh\alpha - \frac{1}{D\alpha}\coth\alpha + G(x_1,x_0) + O(\epsilon), \tag{2.13}$$

using (9.10).

Now we expand the component a around x_1. Therefore we have compute the $O(\epsilon)$ term in (2.13) which requires an expansion of the Green's function. We compute, using (2.11), (2.13) and (9.10),

$$a(x_1+\epsilon y) - a(x_1) =$$

$$= \frac{\alpha}{\sinh\alpha}\frac{c}{\epsilon\xi_\epsilon}\int_{-1}^{1} w^2\left(\frac{x-x_1}{\epsilon}\right)[\tilde{G}(x,x_1+\epsilon y) - \tilde{G}(x,x_1)]\,dx + O(\epsilon^2y^2)$$

$$= I_a + I_b + O(\epsilon^2y^2), \tag{2.14}$$

where

$$\tilde{G}(x,y) = c_1 + e^{\alpha(P-x)}G(x,y), \tag{2.15}$$

$$I_a = \frac{1}{2}(\nabla_z\tilde{G}(x_1,z)|_{z=x_1^+} - \nabla_z\tilde{G}(x_1,z)|_{z=x_1^-})\frac{\epsilon}{6}\int_{\mathbb{R}}(|y-z|-|z|)w^2(z)\,dz$$

$$= [\nabla_z\tilde{G}(x_1,z)|_{z=x_1}]\frac{\epsilon}{6}\int_{\mathbb{R}}(|y-z|-|z|)w^2(z)\,dz$$

$$= \frac{\epsilon\sinh\alpha}{2D\alpha}\int_{\mathbb{R}}(|y-z|-|z|)w^2(z)\,dz,$$

$$I_b = \frac{1}{2}(\nabla_z\tilde{G}(x_1,z)|_{z=x_1^+} + \nabla_z\tilde{G}(x_1,z)|_{z=x_1^-})\epsilon y = < \nabla_z\tilde{G}(x_1,z)|_{z=x_1} > \epsilon y$$

and we have set $P = x_1$ here. (We will need the general case later.)

Next, for the approximate solution, we compute

$$S_\epsilon = \epsilon^2 b_{xx} - \epsilon^2\alpha b_x - b + ab^2$$

$$= \frac{1}{a(x_1)}(\epsilon^2 w_{yy} - w) - \epsilon\alpha\frac{1}{a(x_1)}w_y + \frac{a(x)}{a^2(x_1)}w^2 + O(\epsilon^2)$$

$$= \frac{1}{a(x_1)}\left[\frac{a(x)-a(x_1)}{a(x_1)}w^2 - \epsilon\alpha w_y\right] + O(\epsilon^2) \quad \text{in } H^2_\epsilon(\Omega).$$

When dealing with the operator S_ϵ there is the problem that it is not uniformly invertible for small ϵ. Therefore, to solve the problem $S_\epsilon = 0$, we have to use Liapunov-Schmidt reduction to derive an invertible operator which is suitable for methods from nonlinear analysis. To summarize the argument, the following is done:

We define the approximate kernel as

$$K_{\epsilon,x_1} := \text{span}\left\{ w_y\left(\frac{x-x_1}{\epsilon}\right)\chi\left(\frac{x-x_1^0}{r_0}\right)\right\} \subset H^2\left(\Omega_\epsilon\right),$$

and the approximate co-kernel as

$$C_{\epsilon,x_1} := \text{span}\left\{ w_y\left(\frac{x-x_1}{\epsilon}\right)\chi\left(\frac{x-x_1^0}{r_0}\right)\right\} \subset L^2_\epsilon\left(\Omega_\epsilon\right).$$

The L_2-projection onto C_{ϵ,x_1} is denoted by π_{ϵ,x_1}. Then its orthogonal complement is given by $\pi^\perp_{\epsilon,x_1} := \text{id} - \pi_{\epsilon,x_1}$. Then we introduce the linearized operator

$$\tilde{L}_{\epsilon,x_1} : H^2(\Omega_\epsilon) \to L^2(\Omega_\epsilon)$$

defined by

$$\tilde{L}_{\epsilon,\mathbf{t}} := S'_\epsilon[b_{\epsilon,x_1}]$$

which is the linearization of S_ϵ around the approximate solution. Finally, we consider the linear operator

$$L_{\epsilon,x_1} : K^\perp_{\epsilon,x_1} \to C^\perp_{\epsilon,x_1}$$

defined by

$$L_{\epsilon,x_1} := \pi^\perp_{\epsilon,x_1} \circ \tilde{L}_{\epsilon,x_1}.$$

By an indirect argument it is shown that this operator in invertible and its inverse is bounded uniformly for ϵ small enough.

Then it can be shown that for every $x_1 \in B_{\epsilon^{3/4}}(x_1^0)$ there exists a unique solution $\phi_{\epsilon,x_1} \in K^\perp_{\epsilon,x_1}$ such that

$$S_\epsilon[b_{\epsilon,x_1} + \phi_{\epsilon,x_1}] \in C_{\epsilon,x_1}. \tag{2.16}$$

Finally, in order to solve $S_\epsilon = 0$, it only remains to find $x_1^\epsilon \in B_{\epsilon^{3/4}(x_1^0)}$ such that

$$S_\epsilon[b_{\epsilon,x_1} + \phi_{\epsilon,x_1}] \perp C_{\epsilon,x_1^\epsilon}. \tag{2.17}$$

(For the details of the argument we refer to Section 5 in [27].)

To this end, we have to choose $x_1^\epsilon \in B_{\epsilon^{3/4}}(x_1^0)$ such that $S_\epsilon[b_{\epsilon,x_1^\epsilon}] \perp w_y\chi$ in $L^2(\Omega_\epsilon)$.

First we compute, using (2.14) and (9.10),

$$\begin{aligned}
&\int_{\mathbb{R}} \frac{a(x)-a(x_1)}{a(x_1)} w^2 w_y\,dy \\
&= \int_{-\infty}^0 \frac{a(x_1+\epsilon y)-a(x_1)}{a(x_1)} w^2 w_y\,dy \\
&+ \int_0^\infty \frac{a(x_1+\epsilon y)-a(x_1)}{a(x_1)} w^2 w_y\,dy \\
&= \frac{\epsilon}{a(x_1)} \int_{-\infty}^0 \left[\frac{1}{2D\alpha} - \frac{1}{2D\alpha} e^{\alpha(1+x_1)}\right] y w^2 w_y\,dy \\
&+ \frac{\epsilon}{a(x_1)} \int_0^\infty \left[\frac{1}{2D\alpha} - \frac{1}{2D\alpha} e^{\alpha(-1+x_1)}\right] y w^2 w_y\,dy + O(\epsilon^2)
\end{aligned}$$

$$= \frac{\epsilon e^{\alpha x_1} \sinh \alpha}{6c\alpha} \frac{\int_{\mathbb{R}} w^3}{6D} \left[\frac{1}{2\alpha} \left(e^{\alpha} + e^{-\alpha} \right) e^{\alpha x_1} - \frac{1}{\alpha} \right] + O(\epsilon^2)$$

$$= \frac{\epsilon e^{\alpha x_1} \sinh \alpha}{5Dc\alpha} \left[\frac{\cosh\alpha}{\alpha} e^{\alpha x_1} - \frac{1}{\alpha} \right] + O(\epsilon^2).$$

With the help of this result we calculate

$$0 = a(x_1) \int_{\mathbb{R}} S_\epsilon w_y \, dy$$

$$= \frac{\epsilon e^{\alpha x_1} \sinh \alpha}{5Dc\alpha} \left[\frac{\cosh \alpha}{\alpha} e^{\alpha x_1} - \frac{1}{\alpha} \right] - \epsilon \alpha \int (w_y)^2 \, dy.$$

Using the notation

$$\beta_0 = \frac{6 \int (w_y)^2 \, dy \int w^2 \, dy}{\int w^3 \, dy} = 6, \tag{2.18}$$

this is equivalent to

$$\sinh \alpha \cosh \alpha \, e^{2\alpha x_1} - \sinh \alpha e^{\alpha x_1} - \alpha^3 \beta_0 Dc = O(\epsilon). \tag{2.19}$$

Determining the solution x_1^ϵ of this equation, which is quadratic in $e^{\alpha x_1}$, implies (2.7).

Finally, the solution

$$(a_{\epsilon, x_1^\epsilon}, b_{\epsilon, x_1^\epsilon}) = (a_\epsilon, b_\epsilon)$$

of the system (1.4) with Neumann boundary conditions satisfies all the other properties stated in Theorem 2.1.

□

Note that $x_1^\epsilon \to 0$ as α, $\epsilon \to 0$. This means that as the size of the flow and the activator diffusivity tend to zero, the spike moves to the center of the interval (which is the position of the spike in the absence of the flow). On the other hand, $x_1^\epsilon \to -1$ as $\alpha \to \infty$ and ϵ is small enough. This shows that, if the size of the flow tends to infinity, the spike can move to the left end of the interval.

We observe that the spike has asymmetric shape. The flow breaks the symmetry of the spike. So here we get flow-induced asymmetry. However, this asymmetry occurs not in leading order $O(1)$ but only in order $O(\epsilon)$. This observation will be made rigorous in Section 5 and it will be important when computing eigenfunctions for small eigenvalues in Section 6.

We now change the boundary conditions.

3. Robin boundary conditions (zero flux)

We look for solutions of (1.4) in the interval $\Omega = (-1, 1)$ with no-flux boundary conditions which model zero flux:

$$a_x - \alpha a = b_x - \alpha b = 0, \quad x = -1, \, x = 1. \tag{3.1}$$

Theorem 3.1. *For ϵ small enough, there is a spiky solution (a_ϵ, b_ϵ) of the system (1.4) with Robin boundary conditions (3.1). The shape of this solution is given by*

$$b_\epsilon(x) = \frac{1}{\xi_\epsilon} w \left(\frac{x - x_1^\epsilon}{\epsilon} \right) + O(\epsilon) \text{ in } H_\epsilon^2(-1, 1), \tag{3.2}$$

$$a_\epsilon(x_1^\epsilon) = \xi_\epsilon, \tag{3.3}$$

the amplitude satisfies

$$\xi_\epsilon = \xi_0 + O(\epsilon) \quad \textit{with} \quad \xi_0 = 6c. \tag{3.4}$$

and for the position we have

$$x_1^\epsilon \to x_1^0 \quad \textit{with} \quad x_1^0 = 18Dc\alpha. \tag{3.5}$$

Remarks:

1. In contrast to the case of Neumann boundary conditions we have $x_1^\epsilon > 0$ whatever the size of α is for ϵ small enough. Therefore the spike is located in the right half of the interval in the presence of the flow.

2. Note that $x_1^\epsilon \to 0$ as $\alpha, \epsilon \to 0$. This means that as the size of the flow and the activator diffusivity tend to zero, the position of the spike moves to the center of the interval (which is also the position of the spike in the absence of the flow).

Finally, if α exceeds a certain threshold value, the interior spike ceases from existence. Instead there is a boundary spike at the right boundary.

3. Note that a is a slow function and b is a fast function with respect to the spatial variable x. Therefore, using their asymptotic behavior, we have

$$\frac{c}{\epsilon}\int_{-1}^{1} ab^2\,dx = \frac{c}{\xi_\epsilon}\left(\int_{\mathbb{R}} w^2\,dy\right) + O(\epsilon) = 1 + O(\epsilon). \tag{3.6}$$

Proof of Theorem 3.1:

We now construct a solution which concentrates near x_1^0. The assumptions and definitions for x_1, Ω_ϵ, the cut-off function χ and the approximate solution are the same as in the proof of Theorem 2.1 and are therefore omitted. (Now the formula for ξ_ϵ follows from integrating (2.10) without multiplying by $e^{-\alpha x}$.)

To determine the component a, we use the representation formula given in (9.16) and get

$$a(x_0) = \frac{e^{\alpha x_0}}{2}\int_{-1}^{1} e^{-\alpha x} a(x)\,dx + e^{\alpha x_0}\int_{-1}^{1} f(x) e^{-\alpha x} G(x, x_0)\,dx,$$

where

$$\begin{aligned} f(x) &= \epsilon^{-1} c a(x) b^2(x) = \\ &= \frac{c}{\epsilon \xi_\epsilon} w^2 \chi + O(\epsilon) \quad \text{in } H_\epsilon^2(-1,1) \end{aligned}$$

and $G(x, x_0)$ is given by (9.18). Together with (3.6), this implies

$$\begin{aligned} a(x_0) &= c_1 e^{\alpha x_0} + \frac{c}{\epsilon \xi_\epsilon} e^{\alpha x_0} \int_{-1}^{1} w^2\left(\frac{x - x_1}{\epsilon}\right) e^{-\alpha x} G(x, x_0)\,dx + O(\epsilon) \\ &= c_1 e^{\alpha x_0} + \frac{6c}{a(x_1)} e^{\alpha(x_0 - x_1)} G(x_1, x_0) + O(\epsilon) \\ &= c_1 e^{\alpha x_0} + e^{\alpha(x_0 - x_1)} G(x_1, x_0) + O(\epsilon) \end{aligned} \tag{3.7}$$

for some real constant

$$c_1 = \frac{1}{2}\int_{-1}^{1} e^{-\alpha x} a(x)\,dx.$$

Now we are going to compute the integral in c_1.

Setting $x_1 = x_0$ in (3.7) and using (3.6), we get

$$6c = \frac{1}{2} e^{\alpha x_1} \int_{-1}^{1} e^{-\alpha x} a(x)\, dx + G(x_1, x_1) + O(\epsilon). \tag{3.8}$$

Substituting (3.8) into (3.7) gives

$$\begin{aligned} a(x_0) &= e^{\alpha(x_0 - x_1)}(6c - G(x_1, x_1)) + e^{\alpha(x_0-x_1)} G(x_1, x_0) + O(\epsilon) \\ &= e^{\alpha(x_0-x_1)} \left(6c - \frac{x_1}{D\alpha} - \frac{1}{D\alpha^2} \right) + \frac{\sinh \alpha}{2D\alpha^3} e^{\alpha x_0} + e^{\alpha(x_0-x_1)} G(x_1, x_0) + O(\epsilon), \end{aligned} \tag{3.9}$$

using (9.18).

Now we expand the component a around x_1. We compute, using (3.7), (3.9) and (9.18),

$$\begin{aligned} a(x_1 + \epsilon y) - a(x_1) &= c_1 \alpha e^{\alpha x_1} \epsilon y \\ + \frac{c}{\epsilon a(x_1)} \int_{-1}^{1} w^2 \left(\frac{x - x_1}{\epsilon} \right) & e^{-\alpha x} [e^{\alpha(x_1 + \epsilon y)} G(x, x_1 + \epsilon y) - e^{\alpha x_1} G(x, x_1)]\, dx + O(\epsilon^2 y^2) \\ &= I_a + I_b + O(\epsilon^2 y^2), \end{aligned} \tag{3.10}$$

where

$$\begin{aligned} I_a &= [\nabla_z \tilde{G}(x_1, z)|_{z=x_1}] \frac{\epsilon}{6} \int_{\mathbb{R}} (|y - z| - |z|) w^2(z)\, dz \\ &= \frac{\epsilon}{12D} \int_{\mathbb{R}} (|y - z| - |z|) w^2(z)\, dz, \\ I_b &= < \nabla_z \tilde{G}(x_1, z)|_{z=x_1} > \epsilon y \\ &= \left(6c\alpha - \frac{x_1}{2D} \right) \epsilon y, \\ \tilde{G}(x, z) &= e^{\alpha(z-P)} 6c + e^{\alpha(z-x)} (G(x, z) - G(x, P)) \end{aligned} \tag{3.11}$$

and we have set $P = x_1$ here. (We will need the general case later.)

Now, for the approximate solution $(a_{\epsilon,x_1}, b_{\epsilon,x_1})$, we compute

$$\begin{aligned} S_\epsilon &= \epsilon^2 b_{xx} - \epsilon^2 \alpha b_x - b + ab^2 \\ &= \frac{1}{a(x_1)} (w_{yy} - w) - \epsilon \alpha \frac{1}{a(x_1)} w_y + \frac{a(x)}{a^2(x_1)} w^2 + O(\epsilon^2) \\ &= \frac{1}{a(x_1)} \left[\frac{a(x) - a(x_1)}{a(x_1)} w^2 - \epsilon \alpha w_y \right] + O(\epsilon^2) \quad \text{in } H^2_\epsilon(\Omega). \end{aligned}$$

The framework for Liapunov-Schmidt reduction is the same is in the proof of Theorem 2.1 and we have to find $x_1^\epsilon \in B_{\epsilon^{3/4}}(x_1^0)$ such that $S_\epsilon \perp w_y \chi$ in $L^2(\Omega_\epsilon)$.

First we compute, using (3.10) and (9.18),

$$\begin{aligned} & \int_{\mathbb{R}} \frac{a(x) - a(x_1)}{a(x_1)} w^2 w_y\, dy \\ &= \int_{-\infty}^{0} \frac{a(x_1 + \epsilon y) - a(x_1)}{a(x_1)} w^2 w_y\, dy \\ &\quad + \int_{0}^{\infty} \frac{a(x_1 + \epsilon y) - a(x_1)}{a(x_1)} w^2 w_y\, dy \\ &= \frac{\epsilon}{a(x_1)} \int_{-\infty}^{0} \left[6c\alpha - \frac{x_1}{2D} - \frac{1}{2D\alpha} \right] y w^2 w_y\, dy \end{aligned}$$

$$+\frac{\epsilon}{a(x_1)}\int_0^\infty\left[6c\alpha-\frac{x_1}{2D}+\frac{1}{2D\alpha}\right]yw^2w_y\,dy+O(\epsilon^2)$$
$$=-\frac{\epsilon}{6c}\frac{\int_{\mathbb{R}}w^3}{6D}\left[12Dc\alpha-x_1\right]+O(\epsilon^2)$$
$$=-\frac{\epsilon}{5Dc}\left[12Dc\alpha-x_1\right]+O(\epsilon^2).$$

With the help of this result, we calculate

$$0=a(x_1)\int_{\mathbb{R}}S_\epsilon w_y\,dy$$
$$=-\frac{\epsilon}{5Dc}\left[12Dc\alpha-x_1\right]-\epsilon\alpha\int(w_y)^2\,dy+O(\epsilon^2).$$

This is equivalent to

$$-\frac{\epsilon}{5Dc}\left[12Dc\alpha-x_1\right]-1.2\epsilon\alpha=O(\epsilon^2). \tag{3.12}$$

Determining the solution x_1^ϵ of this equation implies (3.5).

Finally, the solution

$$(a_{\epsilon,x_1^\epsilon},b_{\epsilon,x_1^\epsilon})=(a_\epsilon,b_\epsilon)$$

for the system (1.4) with Robin boundary conditions satisfies all the other properties stated in Theorem 3.1.

□

4. Stability analysis I: Large eigenvalues

In this section, we consider the large eigenvalues of the associated linearized eigenvalue problem.

Let $(a_{\epsilon,},b_\epsilon)$ be the exact one-peaked solution constructed in Sections 2 and 3 for Neumann boundary conditions (zero convective flux) and Robin boundary conditions (zero flux), respectively. We have derived that

$$b_\epsilon=\xi_\epsilon^{-1}w\left(\frac{x-x_1^\epsilon}{\epsilon}\right)+O(\epsilon),\quad a_\epsilon(x_1)=\xi_\epsilon+O(\epsilon), \tag{4.1}$$

where the amplitudes satisfy

$$\xi_\epsilon=\frac{6c\alpha}{e^{\alpha x_1}\sinh\alpha}+O(\epsilon)\quad\text{or}\quad\xi_\epsilon=6c+O(\epsilon)$$

and the positions are given by

$$x_1^ep=\frac{1}{\alpha}\ln\left(1+\sqrt{1+24Dc\alpha^3\coth\alpha}\right)-\frac{1}{\alpha}\ln\left(2\cosh\alpha\right)+O(\epsilon),$$

or

$$x_1^\epsilon=18Dc\alpha+O(\epsilon),$$

respectively.

We linearize (1.3) around (a_ϵ,b_ϵ), using the ansatz $(a_\epsilon+\psi_\epsilon e^{\lambda_\epsilon t},b_\epsilon+\phi_\epsilon e^{\lambda_\epsilon t})$. The eigenvalue problem for $(\psi_\epsilon,\phi_\epsilon)$ then becomes

$$\begin{cases}\epsilon^2\phi_{\epsilon,xx}-\epsilon^2\alpha\phi_{\epsilon,x}-\phi_\epsilon+2b_\epsilon a_\epsilon\phi_\epsilon+\psi_\epsilon b_\epsilon^2=\lambda_\epsilon\phi_\epsilon,\\ D\psi_{\epsilon,xx}-D\alpha\psi_{\epsilon,x}-\frac{c}{\epsilon}\psi_\epsilon b_\epsilon^2-\frac{2c}{\epsilon}a_\epsilon b_\epsilon\phi_\epsilon=\epsilon\lambda_\epsilon\psi_\epsilon,\end{cases} \tag{4.2}$$

where λ_ϵ is some complex number, with the following boundary conditions: In Case 1 (Neumann b.c.) we have

$$\phi_{\epsilon,x}(\pm 1) = \psi_{\epsilon,x}(\pm 1) = 0 \tag{4.3}$$

and in Case 2 (Robin b.c.) we get

$$\phi_{\epsilon,x}(\pm 1) - \alpha\phi_\epsilon(\pm 1) = \psi_{\epsilon,x}(\pm 1) - \alpha\psi_\epsilon(\pm 1) = 0. \tag{4.4}$$

We consider two classes of eigenvalues: The large eigenvalue case, where $\lambda_\epsilon \to \lambda_0 \neq 0$, and the small eigenvalue case, where $\lambda_\epsilon \to 0$.

In this section we will handle the large eigenvalue case. The small eigenvalue case is more involved, and we will analyze it in the following two sections.

Using the cut-off function χ defined in (2.9), we set

$$\tilde{\phi}_\epsilon(x) = \phi_\epsilon(x)\chi\left(\frac{x - x_1^0}{r_0}\right) \in H_\epsilon^2(\Omega). \tag{4.5}$$

Then, from the equation for $\tilde{\phi}_\epsilon$, it is easy to see that

$$\tilde{\phi}_\epsilon(x) = \phi_\epsilon(x) + \text{e.s.t. in} \quad H^2(\Omega_\epsilon), \tag{4.6}$$

where e.s.t. denotes an exponentially small term. For convenience, from now on, we drop the tilde for ϕ_ϵ.

We assume that

$$\|\phi_\epsilon\|_{H_\epsilon^2(\Omega)} \leq C \tag{4.7}$$

if ϵ is small enough. Assume that, after a standard extension of the function $\phi_\epsilon(y)$ from $(\frac{-1-x_1^0}{\epsilon}, \frac{1-x_1^0}{\epsilon})$ to the real line, see for example [4], and using the (4.2) to prove regularity results for ϕ_ϵ, that

$$\phi_\epsilon \to \phi_0(y) \quad \text{in } H^2(\mathbb{R}).$$

Now, using (4.1) and (4.2), we have that $\psi_\epsilon \to \psi_0$ in $H^2(\Omega)$ as $\epsilon \to 0$, where ψ_0 satisfies

$$D\psi_{0,xx} - D\alpha\psi_{0,x} - \gamma\psi_0\delta_{x_1^0} - 2c(\int_{\mathbb{R}} w\phi\, dy)\delta_{x_1^0} = 0, \tag{4.8}$$

where

$$\gamma = \frac{c\int_{\mathbb{R}} w^2}{\xi_0^2} = \frac{6c}{\xi_0^2}, \tag{4.9}$$

where xi_0 has been defined in (2.6) and (3.4), respectively, and $\delta_{x_1^0}$ denotes the Dirac delta distribution located at x_1^0. From now on we drop the subscript 0 for ψ_0 and the superscript 0 for x_1^0. Let

$$\eta = \psi(x_1).$$

Now we will show that

$$\eta = -2\xi_0^2 \frac{\int_{\mathbb{R}} w\phi\, dy}{\int_{\mathbb{R}} w^2\, dy} \tag{4.10}$$

for both types of boundary conditions.

First we consider **Case 1 (Neumann b.c.):**

For $-1 < x < x_1$, we have $\psi_{xx} - \alpha\psi_x = 0$ and $\psi_x(-1) = 0$. Using the fundamental solutions, we get that $\psi = \text{const}$. This implies that

$$\psi(x) = \psi(x_1) = \eta \quad \text{for } -1 < x < x_1. \tag{4.11}$$

Similarly, for $x_1 < x < 1$, we have $\psi_{xx} - \alpha\psi_x = 0$ and $\psi_x(1) = 0$ which implies

$$\psi(x) = \eta \quad \text{for } x_1 < x < 1. \tag{4.12}$$

Now we consider **Case 2 (Robin b.c):**

For $-1 < x < x_1$, we have $(\psi_x - \alpha\psi)_x = 0$ and $\psi_x(-1) - \alpha\psi(-1) = 0$. This implies that

$$\psi_x(x) - \alpha\psi(x) = 0 \quad \text{for } -1 < x < x_1. \tag{4.13}$$

Similarly, for $x_1 < x < 1$, we have $(\psi_x - \alpha\psi)_x = 0$ and $\psi_x(1) - \alpha\psi(1) = 0$ which implies

$$\psi_x(x) - \alpha\psi(x) = 0 \quad \text{for } x_1 < x < 1. \tag{4.14}$$

Since $\psi(x)$ is continuous at $x = x_1$, we get from (4.13) and (4.14) that also $\psi_x(x)$ is continuous at $x = x_1$.

The important fact is that in both cases the function $\psi_x(x)$ is continuous at $x = x_1$. From (4.8) we derive

$$\gamma\eta + 2c\int_{\mathbb{R}} w\phi\, dy = 0 \tag{4.15}$$

since the coefficient of δ_{x_1} must vanish. Together with (4.9) his implies (4.10).

Substituting (4.10) into (4.2), we obtain

$$\phi_{yy} - \phi + 2w\phi - 2\frac{\int_{\mathbb{R}} w\phi\, dy}{\int_{\mathbb{R}} w^2\, dy} w^2 = \lambda\phi. \tag{4.16}$$

Let us recall the following key lemma

Lemma 4.1. [24]*: Consider the nonlocal eigenvalue problem*

$$\phi_{yy} - \phi + 2w\phi - \mu\frac{\int_{\mathbb{R}} w\phi\, dy}{\int_{\mathbb{R}} w^2\, dy} w^2 = \lambda\phi. \tag{4.17}$$

(1) If $\mu < 1$, then there is a positive eigenvalue to (4.17).
(2) If $\mu > 1$, then for any nonzero eigenvalue μ of (4.17) we have

$$Re(\lambda) \le c < 0.$$

(3) If $\mu \neq 1$ and $\lambda = 0$, then

$$\phi = cw_y$$

for some constant c, where w is defined in (2.2).

From Lemma 4.1, we see that the threshold for the stability of large eigenvalues is $\mu = 1$. Since in (4.16) we have $\mu = 2 > 1$, Case 2 of Lemma 4.1 applies and we derive that the eigenvalues of (4.16) all satisfy $\mathrm{Re}(\lambda) \le c < 0$. By a perturbation argument (see for example [27]) we derive that this estimate also holds for ϵ small enough.

In summary, we have arrived at the following proposition:

Proposition 4.2. *Let $\lambda_\epsilon \to \lambda_0 \neq 0$ be an eigenvalue of (4.2). Then $Re(\lambda_\epsilon) \le c < 0$, for some $c < 0$ independent of ϵ.*

This finishes the study of large eigenvalues.

To conclude this section, we study the conjugate L^* to the linear operator L. It is easy to see that L^* is given by

$$L^*\phi = \phi_{yy} - \phi + 2w\phi - 2\frac{\int_{\mathbb{R}} w^2\phi\, dy}{\int_{\mathbb{R}} w^2\, dy} w, \tag{4.18}$$

where

$$\phi \in H^2(\mathbb{R}).$$

We obtain the following result.

Lemma 4.3.

$$Ker(L) = X_0, \tag{4.19}$$

where

$$X_0 = span\,\{w_y(y)\}$$

and w is defined in (2.2). Further,

$$Ker(L^*) = X_0. \tag{4.20}$$

Proof: First we note that (4.19) follows from Lemma 4.1 (3).

To prove (4.20), we multiply the equation $L^*\phi = 0$ by w and integrate over the real line. After integration by parts we obtain

$$\int_{\mathbb{R}} w^2\phi\, dy = 0.$$

Thus the non-local term vanishes and we have

$$L_0\phi := \Delta\phi - \phi + 2w\phi = 0, \tag{4.21}$$

This implies that $\phi \in X_0$. Further, since w_y is an odd function it is easy to see that $L^*\phi = 0$ for all $\phi \in X_0$. This implies (4.20). □

As a consequence of Lemma 4.3, we have a result on the restriction of the operator L to the orthogonal complements of X_0:

Lemma 4.4. *The operator*

$$L : X_0^\perp \cap H^2(\mathbb{R}) \to X_0^\perp \cap L^2(\mathbb{R})$$

is invertible. Moreover, L^{-1} is bounded.

Proof: This follows from the Fredholm Alternatives Theorem and Lemma 4.3.

□

5. Further improvement of the solutions

As a preparation for the computation of the small eigenvalues of the problem (4.2), in this section we further improve our expansion for the solutions derived in Sections 2 and 3 for Neumann and Robin boundary conditions, respectively.

Using the analysis in Section 4, in particular Lemma 4.3, we get in the limit $\lambda_\epsilon \to \lambda_0 = 0$ that

$$\phi_\epsilon \to \phi \quad \text{in } H^2(\mathbb{R}),$$

where $L\phi = 0$. Hence Lemma 4.1 implies that $\phi = cw_y(y)$ for some real constant c. This suggests that the first term in the expansion of $\phi_\epsilon(y)$ is $aw_y(y)$ for some suitable constant a. We need to expand the eigenfunction ϕ_ϵ up to the order $O(\epsilon^2)$-term. To this end, we first expand the first component b_ϵ of the exact solution up to order $O(\epsilon^2)$.

More precisely, we will show that

$$b_\epsilon = \xi_\epsilon^{-1}(w + w_1 + w_2 + w_3 + w_4)\chi + \phi^\perp = \xi_\epsilon^{-1}(w + \epsilon w_1^0 + \epsilon^2 w_2^0 + \epsilon w_3^0 + \epsilon^2 w_4^0)\chi + \phi^\perp, \tag{5.1}$$

where we set $w_1 = \epsilon w_1^0$, $w_2 = \epsilon^2 w_2^0$, $w_3 = \epsilon w_3^0$, $w_4 = \epsilon^2 w_4^0$, $\xi_\epsilon = \xi_0 + O(\epsilon)$ and $\phi^\perp \in C^\perp_{\epsilon, x_1^\epsilon}$, $\|\phi^\perp\|_{H^2(\mathbb{R}^2)} = O(\epsilon^3)$. Further, w_1^0, w_4^0 are odd and w, w_2^0, w_3^0 are even functions which will be introduce in this section.

First we consider **Neumann boundary conditions**.

Recall from (2.15) that

$$\tilde{G}(x,y) = c_1 + e^{\alpha(P-x)}G(x,y).$$

Next we consider **Robin boundary conditions**.

Recall from (3.11) that

$$\tilde{G}(x,y) = e^{\alpha(y-P)}6c + e^{\alpha(y-x)}(G(x,y) - G(x,P)).$$

We define the average gradient for the function $\tilde{G}$, taken with respect to the second argument, as

$$< \nabla\tilde{G}(x,x) > := < \nabla_z\tilde{G}(x,z)|_{z=x} > = \frac{1}{2}\left(\tilde{G}_z(x,z^+) + \tilde{G}_z(x,z^-)\right)|_{z=x}, \tag{5.2}$$

where $\tilde{G}_z(x,z^+)$ denotes the right-hand partial derivative etc. Half the jump of the gradient, taken with respect to the second argument, is denoted as

$$[\nabla\tilde{G}(x,x)] := [\nabla_z\tilde{G}(x,z)|_{z=x}] = \frac{1}{2}\left(\tilde{G}_z(x,z^+) - \tilde{G}_z(x,z^-)\right)|_{z=x}. \tag{5.3}$$

There are two types of second gradients to consider. The first type is a double derivative with respect to the second argument, denoted by $\nabla^2\tilde{G}$. The second type is a single derivative with respect to each of the first and second arguments, denoted by $\nabla\nabla\tilde{G}$. For both types of second gradients we now define the average and half the jump as follows:

$$< \nabla^2\tilde{G}(x,x) > := < \nabla_z^2\tilde{G}(x,z) > |_{z=x} > = \frac{1}{2}\left(\tilde{G}_{zz}(x,z^+) + \tilde{G}_{zz}(x,z^-)\right)_{z=x}, \tag{5.4}$$

$$[\nabla^2\tilde{G}(x,x)] := [\nabla_z^2\tilde{G}(x,z) > |_{z=x}] = \frac{1}{2}\left(\tilde{G}_{zz}(x,z^+) - \tilde{G}_{zz}(x,z^-)\right)_{z=x}, \tag{5.5}$$

$$< \nabla\nabla\tilde{G}(x,x) > := < \nabla_x\nabla_z\tilde{G}(x,z) > |_{z=x} > = \frac{1}{2}\left(\tilde{G}_{xz}(x,z^+) + \tilde{G}_{xz}(x,z^-)\right)_{z=x}, \tag{5.6}$$

$$[\nabla\nabla\tilde{G}(x,x)] := [\nabla_x\nabla_z\tilde{G}(x,z) > |_{z=x}] = \frac{1}{2}\left(\tilde{G}_{xz}(x,z^+) - \tilde{G}_{xz}(x,z^-)\right)_{z=x}. \tag{5.7}$$

Now we expand the solution b_ϵ up to order ϵ^2.

Let $w_1^0 \in X_0^\perp$ be the unique solution of the problem

$$w_{1,yy}^0 - w_1^0 + 2ww_1^0 - 2\underbrace{\frac{\int ww_1^0\,dy}{\int w^2\,dy}}_{=0 \text{ since } w_1^0 \text{ is odd}} w^2 = \alpha w_y - yw^2\frac{< \nabla\tilde{G}(x_1^0,x_1^0) >}{a(x_1^0)}. \tag{5.8}$$

Note that (5.8) has a unique solution which follows from Lemma 4.4 using the fact that

$$\int_{\mathbb{R}} \left[\alpha w_y - y w^2 \frac{< \nabla \tilde{G}(x_1^0, x_1^0) >}{a(x_1^0)} \right] w_y \, dy = 0. \tag{5.9}$$

Statement (5.9) is equivalent to

$$\frac{< \nabla \tilde{G}(x_1^0, x_1^0) >}{a(x_1^0)} = -\frac{1}{2}\alpha.$$

This statement follows by a suitable choice of spike position (see Sections 2 and 3). An explicit calculation gives $w_1^0 = \frac{\alpha}{2} y w$. We remark that w_1^0 is an odd function in y.

Let $w_2^0 \in X_0^\perp$ be the unique solution of the problem

$$w_{2,yy}^0 - w_2^0 + 2ww_2^0 - 2\frac{\int ww_2^0\,dy}{\int w^2\,dy} w^2$$

$$= \alpha w_{1,y}^0 - 2yww_1^0 \frac{< \nabla \tilde{G}(x_1^0, x_1^0) >}{a(x_1^0)} - \frac{1}{2} y^2 w^2 \frac{< \nabla^2 \tilde{G}(x_1^0, x_1^0) >}{a(x_1^0)}$$

$$-(w_1^0 + w_3^0)^2 + \frac{\int (w_1^0)^2\,dy + \int (w_3^0)^2\,dy}{\int w^2\,dy} w^2 - 4\left(\frac{\int ww_3^0\,dy}{\int w^2\,dy}\right)^2 w^2 + 4\frac{\int ww_3^0}{\int w^2} ww_3^0. \tag{5.10}$$

Note that (5.10) has a unique solution by Lemma 4.4 since its r.h.s is an even function and so is orthogonal to w_y. We remark that w_2^0 is an even function in y.

Let $w_3^0 \in X_0^\perp$ be the unique solution of the problem

$$w_{3,yy}^0 - w_3^0 + 2ww_3^0 - 2\frac{\int ww_3^0\,dy}{\int w^2\,dy} w^2$$

$$= -w^2 \frac{[\nabla \tilde{G}(x_1^\epsilon, x_1^\epsilon)]}{a(x_1^\epsilon)} \frac{1}{\int_{\mathbb{R}^2} w^2(z)\,dz} \int_{\mathbb{R}^2} (|y-z| - |z|) w^2(z)\,dz. \tag{5.11}$$

Note that (5.11) has a unique solution which follows from Lemma 4.4 since r.h.s. is an even function and so is orthogonal to w_y. We remark that w_3^0 is an even function in y.

Let $w_4^0 \in X_0^\perp$ be the unique solution of the problem

$$w_{4,yy}^0 - w_4^0 + 2ww_4^0 - 2 \underbrace{\frac{\int ww_4^0\,dy}{\int w^2\,dy}}_{=0 \text{ since } w_4^0 \text{ is odd}} w^2$$

$$= -yw^2 \frac{[\nabla^2 \tilde{G}(x_1^0, x_1^0)]}{a(x_1^0)} \frac{\int_{\mathbb{R}^2} 2w_3^0(z) w(z)\,dz}{\int_{\mathbb{R}^2} w^2(z)\,dz} - 2yww_3^0 \frac{[\nabla \tilde{G}(x_1^0, x_1^0)]}{a(x_1^0)}$$

$$+\pi_{\epsilon, x_1^0}^\perp \left[\alpha w_{3,y}^0 - w^2 \frac{[\nabla \tilde{G}(x_1^\epsilon, x_1^\epsilon)]}{a(x_1^\epsilon)} \frac{1}{\int_{\mathbb{R}^2} w^2(z)\,dz} \int_{\mathbb{R}^2} \frac{1}{2} \mathrm{sgn}(y-z) |y-z|^2 w^2(z)\,dz + 4\frac{\int ww_3^0}{\int w^2} ww_1^0 \right]$$

$$-\epsilon^{-1} \pi_{\epsilon, x_1^\epsilon}^\perp \left[-\alpha w_y + yw^2 \frac{< \nabla \tilde{G}(x_1^\epsilon, x_1^\epsilon)]}{a(x_1^\epsilon)} \right] + \epsilon^{-1} \pi_{\epsilon, x_1^0}^\perp \underbrace{\left[-\alpha w_y + yw^2 \frac{< \nabla \tilde{G}(x_1^0, x_1^0)]}{a(x_1^0)} \right]}_{=0} := f_1(y), \tag{5.12}$$

where $f_1(y)$ represents the total r.h.s. of (5.12). Note that (5.12) has a unique solution which follows from Lemma 4.4 since $f_1(y)$ is orthogonal to w_y by the definition of the projection $\pi_{\epsilon, x_1^0}^\perp$. We remark that $f_1(y)$ is an odd function and so w_4^0 is also an odd function.

Remark: The projection, which is an odd function, satisfies

$$\pi_{\epsilon,x_1^\epsilon}\left[\epsilon\alpha w_y-\epsilon y w^2\frac{<\nabla\tilde{G}(x_1^\epsilon,x_1^\epsilon)>}{a(x_1^\epsilon)}\right]-\underbrace{\pi_{\epsilon,x_1^0}\left[\epsilon\alpha w_y-\epsilon y w^2\frac{<\nabla\tilde{G}(x_1^0,x_1^0)>}{a(x_1^0)}\right]}_{=0}$$

$$-\pi_{\epsilon,x_1^0}\left[\alpha w^0_{3,y}-w^2\frac{[\nabla^2\tilde{G}(x_1^0,x_1^0)]}{a(x_1^0)}\frac{1}{\int_{\mathbb{R}^2}w^2(z)\,dz}\int_{\mathbb{R}^2}\frac{1}{2}\mathrm{sgn}(y-z)|y-z|^2\,dz\right]\epsilon^2=O(\epsilon^2).$$

This relation is included in the equation which is solved by the spike position x_1^ϵ. Because of the non-degeneracy of $\tilde{G}$, namely the condition $<\nabla_{x_1^2}\tilde{G}(x_1^0,x_1^0)>\neq 0$, we will get $|x_1^\epsilon-x_1^0|=O(\epsilon)$. Formally, this equation determines the ϵ order term of x_1^ϵ.

Now it follows that $S_\epsilon[(w+\epsilon w_1^0+\epsilon^2 w_2^0+\epsilon w_3^0+\epsilon^2 w_4^0)\chi]=O(\epsilon^3)$ since by the definition of w and w_i^0, $i=1,2,3,4$ all the terms up to order ϵ^3 cancel. Using Liapunov-Schmidt reduction, in particular the elliptic estimates for the solution of the nonlinear problem as indicated in the proof of Theorem 2.1, we finally have

$$b_\epsilon=\xi_\epsilon^{-1}(w+w_1+w_2+w_3+w_4)\chi+\phi^\perp=\xi_\epsilon^{-1}(w+\epsilon w_1^0+\epsilon^2 w_2^0+\epsilon w_3^0+\epsilon^2 w_4^0)\chi+\phi^\perp,$$

where $\xi_\epsilon=\xi_1^)+O(\epsilon)$ and $\phi^\perp\in C^\perp_{\epsilon,x_1^\epsilon}$, $\|\phi^\perp\|_{H^2_\epsilon(\Omega)}=O(\epsilon^3)$. Further, w_1^0, w_4^0 are odd and w, w_2^0, w_3^0 are even functions.

6. Stability analysis II: Small eigenvalues

As we shall prove, the small eigenvalues are of the order $O(\epsilon^2)$. Let us define

$$\tilde{b}_\epsilon(x)=\chi\left(\frac{x-x_1^0}{r_0}\right)b_\epsilon(x), \tag{6.1}$$

where χ has been defined before (4.5). Then it is easy to see that

$$\tilde{b}_\epsilon(x)=b_\epsilon(x)+\text{e.s.t.}\quad \text{in } H^2_\epsilon(\Omega). \tag{6.2}$$

From the defining equations for w and w_i^0 let us define the following identities which will be used in the stability proof.

Taking derivatives w.r.t. y in (5.8) gives

$$w^0_{1,yyy}-w^0_{1,y}+2w_y w_1^0+2ww^0_{1,y}=\alpha w_{yy}+\frac{\alpha}{2}(w^2+2yww_y). \tag{6.3}$$

Taking derivatives w.r.t. y in (5.10) gives

$$w^0_{2,yyy}-w^0_{2,y}+2w_y w_2^0+2ww^0_{2,y}-4\frac{\int ww_2^0\,dy}{\int w^2\,dy}ww_y$$

$$=\alpha w^0_{1,yy}-2(yw_yw_1^0+yww^0_{1,y}+ww_1^0)\frac{<\nabla\tilde{G}(x_1^0,x_1^0)>}{a(x_1^0)}-(y^2ww_y+yw^2)\frac{<\nabla^2\tilde{G}(x_1^0,x_1^0)>}{a(x_1^0)}$$

$$-2(w_1^0+w_3^0)(w_1^0+w_3^0)_y+\frac{\int(w_1^0)^2\,dy+\int(w_3^0)^2\,dy}{\int w^2\,dy}2ww_y-8\left(\frac{\int ww_3^0\,dy}{\int w^2\,dy}\right)^2ww_y$$

$$+4\frac{\int ww_3^0}{\int w^2}(w_yw_3^0+ww^0_{3,y}). \tag{6.4}$$

Taking derivatives w.r.t. y in (5.11) gives

$$w^0_{3,yyy} - w^0_{3,y} + 2w_y w^0_3 + 2ww^0_{3,y} - 4\frac{\int ww^0_3\,dy}{\int w^2\,dy} ww_y$$

$$= -2ww_y \frac{[\nabla \tilde{G}(x^\epsilon_1, x^\epsilon_1)]}{a(x^\epsilon_1)} \frac{1}{\int_{\mathbb{R}^2} w^2(z)\,dz} \int_{\mathbb{R}^2} (|y-z| - |z|) w^2(z)\,dz$$

$$-w^2 \frac{[\nabla \tilde{G}(x^\epsilon_1, x^\epsilon_1)]}{a(x^\epsilon_1)} \frac{1}{\int_{\mathbb{R}^2} w^2(z)\,dz} \int_{\mathbb{R}^2} (|y-z| - |z|) 2w(z) w_z(z)\,dz, \tag{6.5}$$

where we have used

$$\frac{d}{dy}\int_{\mathbb{R}^2} |y-z| w^2(z)\,dz = \int_{\mathbb{R}^2} (-\frac{d}{dz}|y-z|) w^2(z)\,dz = \int_{\mathbb{R}^2} |y-z| 2w(z) w_z(z)\,dz,$$

$$\frac{d}{dy}\int_{\mathbb{R}^2} |z| w^2(z)\,dz = 0.$$

Taking derivatives w.r.t. y in (5.12) gives

$$w^0_{4,yyy} - w^0_{4,y} + 2ww^0_{4,y} + 2w_y w^0_4 - 4\frac{\int ww^0_4\,dy}{\int w^2\,dy} ww_y$$

$$= \frac{d}{dy} f_1(y). \tag{6.6}$$

Note that $\frac{d}{dy} f_1(y)$ is an even function and so $w^0_{4,y}$ is also even. Note that $w^0_{4,y}$ is an even function and it can be handled by adding an even correction of order ϵ^2 to the eigenfunction (see the analysis below).

Note that

$$\tilde{b}_\epsilon \sim \xi_\epsilon^{-1} w(y)\chi \quad \text{in } H^2_\epsilon(\Omega)$$

and $\tilde{b}_\epsilon(x)$ satisfies

$$\epsilon^2 \tilde{b}_{\epsilon,xx} - \epsilon^2 \alpha \tilde{b}_{\epsilon,x} - \tilde{b}_\epsilon + \tilde{b}^2_\epsilon a_\epsilon = \text{e.s.t.} \quad \text{in } H^2_\epsilon(\Omega). \tag{6.7}$$

Taking derivatives w.r.t. x, we get

$$\begin{cases} \epsilon^2 \tilde{b}_{\epsilon,xxx} - \epsilon^2 \alpha \tilde{b}_{\epsilon,xx} - \tilde{b}_{\epsilon,x} + 2\tilde{b}_\epsilon a_\epsilon \tilde{b}_{\epsilon,x} + \tilde{b}^2_\epsilon a_{\epsilon,x} + \text{e.s.t.} = 0, \\ \tilde{b}_{\epsilon,x}(\pm 1) = 0 \quad \text{or} \quad \tilde{b}_{\epsilon,x}(\pm 1) - \alpha \tilde{b}_\epsilon(\pm 1) = 0 \end{cases} \tag{6.8}$$

in Case 1 or Case 2, respectively.

Let us now decompose

$$\phi_\epsilon = \chi(w_y + \epsilon w^0_{1,y} + \epsilon^2 w^0_{2,y} + \epsilon w^0_{3,y} + \epsilon^2 w^0_{4,y}) + \phi^\perp_\epsilon + O(\epsilon^2), \tag{6.9}$$

where

$$\phi^\perp_\epsilon \perp X_0 = \text{span}\,\{\chi w_y\} \subset H^2(\Omega_\epsilon),$$

and $\Omega_\epsilon = \left(\frac{-1-x_1}{\epsilon}, \frac{1-x_1}{\epsilon}\right)$.

Our proof will consist of two steps. First we will show that $\|\phi^\perp_\epsilon - \epsilon\phi^\perp_1 - \epsilon^2\phi^\perp_2\|_{H^2(\Omega_\epsilon)} = O(\epsilon^3)$ for suitably chosen even functions $\phi^\perp_1$, $\phi^\perp_2 \in H^2(\Omega_\epsilon)$ such that $\|\phi^\perp_1\|_{H^2(\Omega_\epsilon)}$, $\|\phi^\perp_2\|_{H^2(\Omega_\epsilon)} \le C$. Second we will derive the asymptotic behavior of the eigenvalue λ_ϵ as $\lambda \to 0$.

As a preparation, we need to compute $L\left[\left(w_y + \epsilon w^0_{1,y} + \epsilon^2 w^0_{2,y} + \epsilon w^0_{3,y} + \epsilon^2 w^0_{4,y}\right)\chi\right]$, where

$$L\phi = \phi_{yy} - \epsilon\alpha\phi_y - \phi + 2b_\epsilon a_\epsilon \phi + \psi b^2_\epsilon$$

for $\phi \in H^2_\epsilon(\Omega)$, the functions w, w_1^0, w_2^0, w_3^0, w_4^0 have been defined in (2.2), (5.8), (5.10), (5.11), (5.12) respectively, and ψ is derived by solving the second equation of (4.2).

Substituting the decomposition $\phi = \left(w_y + \epsilon w^0_{1,y} + \epsilon^2 w^0_{2,y} + \epsilon w^0_{3,y} + \epsilon^2 w^0_{4,y}\right)\chi$ into (4.2) and using (5.8), (5.10), (5.11), (5.12), (6.3), (6.4), (6.5), we have

$$
\begin{aligned}
L\phi &= \phi_{yy} - \epsilon\alpha\phi_y - \phi \\
&+2\chi(w+\epsilon w_1^0+\epsilon^2 w_2^0+\epsilon w_3^0+\epsilon^2 w_4^0)\left(1+\frac{2\epsilon\int ww_3^0+2\epsilon^2\int ww_2^0\,dy+\epsilon^2\int(w_1^0)^2+\epsilon^2\int(w_3^0)^2}{\int w^2\,dy}\right)^{-1}\phi \\
&+2\epsilon y\frac{<\nabla\tilde{G}(x_1^\epsilon,x_1^\epsilon)>}{\xi_\epsilon}\chi(w+\epsilon w_1^0+\epsilon w_3^0)\phi+2\epsilon^2\frac{1}{2}y^2\frac{<\nabla^2\tilde{G}(x_1^0,x_1^0)>}{\xi_0}\chi w w_y \\
&-2\epsilon\chi(w+\epsilon w_1^0+\epsilon w_3^0)\phi\frac{[\nabla\tilde{G}(x_1^\epsilon,x_1^\epsilon)]}{\xi_\epsilon}\frac{1}{\int_{\mathbb{R}^2}w^2(z)\,dz}\int_{\mathbb{R}^2}(|y-z|-|z|)w^2(z)\,dz \\
&-2\epsilon^2\chi w w_y\frac{[\nabla^2\tilde{G}(x_1^0,x_1^0)]}{\xi_\epsilon}\frac{1}{\int_{\mathbb{R}^2}w^2(z)\,dz}\int_{\mathbb{R}^2}\frac{1}{2}\mathrm{sgn}(y-z)|y-z|^2w^2(z)\,dz \\
&-2\underbrace{\frac{\int(w+\epsilon w_1^0+\epsilon^2 w_2^0+\epsilon w_3^0+\epsilon^2 w_4^0)\phi_\epsilon\,dy}{\int(w)^2\,dy}}_{=O(\epsilon^3)}\chi(w+\epsilon w_1^0+\epsilon^2 w_2^0+\epsilon w_3^0+\epsilon^2 w_4^0)^2 \\
&+\epsilon y\nabla\psi(x_1^\epsilon)\frac{w^2}{\xi_\epsilon^2}+O(\epsilon^3) \\
&= (w_{yyy}-w_y+2ww_y) \\
&+\epsilon\left(w^0_{1,yyy}-w^0_{1,y}+2w_yw_1^0+2ww^0_{1,y}\right) \\
&+\epsilon\left(-\alpha w_{yy}+2yww_y\frac{<\nabla\tilde{G}(x_1^0,x_1^0)>}{\xi_\epsilon}\right) \\
&+\epsilon^2\left(w^0_{2,yyy}-w^0_{2,y}+2w_yw_2^0+2ww^0_{2,y}-4\frac{\int ww_2^0\,dy}{\int w^2\,dy}ww_y\right) \\
&-\epsilon^2\left(\alpha w^0_{1,yy}-2(yw_yw_1^0+yww^0_{1,y})\frac{<\nabla\tilde{G}(x_1^0,x_1^0)>}{\xi_0}-(y^2ww_y)\frac{<\nabla^2\tilde{G}(x_1^0,x_1^0)>}{\xi_0}\right) \\
&-\epsilon^2\Bigg(-2(w_1^0+w_3^0)(w_1^0+w_3^0)_y+\frac{\int(w_1^0)^2\,dy+\int(w_3^0)^2\,dy}{\int w^2\,dy}2ww_y-8\left(\frac{\int ww_3^0}{\int w^2}\right)ww_y \\
&\qquad+4\frac{\int ww_3^0}{\int w^2}(w_yw_3^0+ww^0_{3,y})\Bigg) \\
&+\epsilon\left(w^0_{3,yyy}-w^0_{3,y}+2w_yw_3^0+2ww^0_{3,y}-4\frac{\int ww_3^0\,dy}{\int w^2\,dy}ww_y\right) \\
&+\epsilon 2ww_y\frac{[\nabla\tilde{G}(x_1^\epsilon,x_1^\epsilon)]}{\xi_\epsilon}\frac{1}{\int_{\mathbb{R}^2}w^2(z)\,dz}\int_{\mathbb{R}^2}(|y-z|-|z|)w^2(z)\,dz \\
&+\epsilon w^2\frac{[\nabla\tilde{G}(x_1^\epsilon,x_1^\epsilon)]}{\xi_\epsilon}\frac{1}{\int_{\mathbb{R}^2}w^2(z)\,dz}\int_{\mathbb{R}^2}(|y-z|-|z|)2w(z)w_z(z)\,dz \\
&+\epsilon^2\left(w^0_{4,yyy}-w^0_{4,y}+2ww^0_{4,y}+2w_yw_4^0-4\frac{\int ww_4^0\,dy}{\int w^2\,dy}ww_y\right)
\end{aligned}
$$

$$+\epsilon^2 g_1(y)+\epsilon y\nabla\psi_\epsilon(x_1^\epsilon)\frac{w^2}{\xi_\epsilon^2}+O(\epsilon^3)$$

$$=-\epsilon w^2\frac{<\nabla\tilde G(x_1^0,x_1^0)>}{\xi_0}-\epsilon^2\alpha\frac{<\nabla\tilde G(x_1^0,x_1^0)>}{\xi_0}yw^2-\epsilon^2\frac{<\nabla^2\tilde G(x_1^0,x_1^0)>}{\xi_0}yw^2-\epsilon^2\frac{<\nabla\nabla\tilde G(x_1^0,x_1^0)>}{\xi_0}yw^2$$

$$-\epsilon^2\frac{d}{dy}f_1(y)+\epsilon^2 g_1(y)+O(\epsilon^3), \tag{6.10}$$

where the odd function $f_1(y)$ has been defined in (5.12) and the even function $g_1(y)$ is defined as

$$g_1(y):=-2yww_y\frac{[\nabla\tilde G(x_1^0,x_1^0)]}{\xi_0}\frac{\int_{\mathbb{R}^2}2w_3^0(z)w(z)\,dz}{\int_{\mathbb{R}^2}w^2(z)\,dz}-(2yw_yw_3^0+2yww_{3,y}^0)\frac{[\nabla\tilde G(x_1^0,x_1^0)]}{\xi_0}$$

$$+\pi^\perp_{\epsilon,x_1^0}\left[\alpha w^0_{3,yy}-2ww_y\frac{[\nabla^2\tilde G(x_1^0,x_1^0)]}{\xi_0}\frac{1}{\int_{\mathbb{R}^2}w^2(z)\,dz}\int_{\mathbb{R}^2}\frac{1}{2}\mathrm{sgn}(y-z)|y-z|^2w^2(z)\,dz\right]$$

$$+\pi^\perp_{\epsilon,x_1^0}\left[4\frac{\int ww_3^0}{\int w^2}(w_yw_1^0+ww_{1,y}^0)\right]$$

$$-\pi^\perp_{\epsilon,x_1^0}\left[w^2\frac{[\nabla^2\tilde G(x_1^0,x_1^0)]}{\xi_0}\frac{1}{\int_{\mathbb{R}^2}w^2(z)\,dz}\int_{\mathbb{R}^2}\mathrm{sgn}(y-z)|y-z|^2w(z)w_z(z)\,dz\right]$$

$$-\pi^\perp_{\epsilon,x_1^\epsilon}\epsilon^{-1}\left[2yww_y\frac{<\nabla\tilde G(x_1^\epsilon,x_1^\epsilon)]}{\xi_\epsilon}\right]+\pi^\perp_{\epsilon,x_1^0}\epsilon^{-1}\left[2yww_y\frac{<\nabla\tilde G(x_1^0,x_1^0)]}{\xi_0}\right]. \tag{6.11}$$

The last equality sign in (6.10) holds since in the previous expression the first line vanishes by the definition of w. Lines 2-3 equal $-\epsilon w^2\frac{<\nabla G(x_1^0,x_1^0)>}{\xi_0}$ by (6.3). Lines 4-7 equal

$$-\epsilon^2\alpha\frac{<\nabla\tilde G(x_1^0,x_1^0)>}{\xi_0}yw^2-\epsilon^2\frac{<\nabla^2\tilde G(x_1^0,x_1^0)>}{\xi_0}yw^2$$

by (6.4). Lines 8-10 vanish by (6.5).

Here we have used

$$\frac{\psi(x_1^0)}{\xi_0^2}=-\frac{2\int(w+\epsilon w_1^0+\epsilon^2w_2^0+\epsilon w_3^0+\epsilon^2w_4^0+O(\epsilon^3))(w_y+\epsilon w_{1,y}^0+\epsilon^2w_{2,y}^0+\epsilon w_{3,y}^0+\epsilon^2w_{4,y}^0+O(\epsilon^3))\,dy}{\int(w+\epsilon w_1^0++\epsilon^2w_2^0+\epsilon w_3^0+\epsilon^2w_4^0+O(\epsilon^3))^2\,dy}\xi_0^2$$

$$=O(\epsilon^3)$$

which follows by arguments as in Section 4. Further, we have used

$$\nabla\psi(x_1^\epsilon)=\nabla\psi(x_1^0)+O(\epsilon^2)$$

$$=\left(\frac{\xi_0}{\int w^2}\right)\int_{(-x_1-1)/\epsilon}^{(-x_1+1)/\epsilon}<\nabla_x\tilde G(x_1^0,x_1^0)>\left(\underbrace{\psi(x_1^0)}_{=O(\epsilon^2)}\frac{w^2(z)}{\xi_0^2}+2w(z)w_z(z)\right)dz+O(\epsilon^2)$$

$$=\epsilon\left(\frac{\xi_0}{\int w^2}\right)<\nabla\nabla\tilde G(x_1^0,x_1^0)>\int 2zww_z\,dz+O(\epsilon^2)$$

$$=-\epsilon\xi_0<\nabla\nabla\tilde G(x_1^0,x_1^0)>+O(\epsilon^2).$$

The derivation of this formula linking $\nabla\psi(x_1^0)$ with $\nabla\nabla\tilde G(x_1^0,x_1^0)$ is delayed to Appendix A (Section 9) where it will be given for both Neumann and Robin boundary conditions (see formulas (9.27) and (9.38).

Step 1.

Substituting the eigenfunction expansion given in (6.9) into the linear operator L, we get

$$L\left[\left(w_y+\epsilon w^0_{1,y}+\epsilon^2 w^0_{2,y}+\epsilon w^0_{3,y}+\epsilon^2 w^0_{4,y}\right)\chi+\phi_\epsilon^\perp\right]$$
$$=\lambda_\epsilon\left(\left(w_y+\epsilon w^0_{1,y}+\epsilon^2 w^0_{2,y}+\epsilon w^0_{3,y}+\epsilon^2 w^0_{4,y}\right)\chi+\phi_\epsilon^\perp\right)+O(\epsilon^3). \tag{6.12}$$

Therefore $\phi_\epsilon^\perp$ satisfies the equation

$$L[\phi_\epsilon^\perp]-\lambda_\epsilon\phi_\epsilon^\perp=-(L-\lambda_\epsilon)[\left(w_y+\epsilon w^0_{1,y}+\epsilon^2 w^0_{2,y}+\epsilon w^0_{3,y}+\epsilon^2 w^0_{4,y}\right)\chi$$
$$=\lambda_\epsilon\left(w_y+\epsilon w^0_{1,y}+\epsilon^2 w^0_{2,y}+\epsilon w^0_{3,y}+\epsilon^2 w^0_{4,y}\right)\chi$$
$$+\epsilon\frac{<\nabla\tilde G(x_1^0,x_1^0)>}{\xi_0}w^2+\epsilon^2\frac{\alpha}{2}\frac{<\nabla\tilde G(x_1^0,x_1^0)>}{\xi_0}yw^2+\epsilon^2\frac{<\nabla^2\tilde G(x_1^0,x_1^0)>}{\xi_0}yw^2+\epsilon^2\frac{<\nabla\nabla\tilde G(x_1^0,x_1^0)>}{\xi_0}yw^2$$
$$+\epsilon^2\frac{d}{dy}f_1(y)-\epsilon^2 g_1(y)+O(\epsilon^3).$$

We derive the following estimate, using a projection as in Liapunov-Schmidt reduction for the linearised operator,

$$\|\phi_\epsilon^\perp-\epsilon\phi_1^\perp\epsilon^2\phi_2^\perp\|_{H^2(\Omega_\epsilon)}=O(\epsilon^3+|\lambda_\epsilon|\|\phi_\epsilon\|_{H^2(\Omega_\epsilon)}). \tag{6.13}$$

Here $\phi_1^\perp$ is the unique even function in $H^2(\mathbb{R})$ which satisfies

$$\phi_{1,yy}^\perp-\phi_1^\perp+2w\phi_1^\perp-2\frac{\int w\phi_1^\perp\,dy}{\int w^2}w^2=\frac{<\nabla\tilde G(x_1^0,x_1^0)>}{\xi_0}w^2$$

and is given by

$$\phi_1^\perp=-\frac{<\nabla\tilde G(x_1^0,x_1^0)>}{\xi_0}w. \tag{6.14}$$

Further, $\phi_2^\perp\in H^2(\mathbb{R})$ is the unique even function which satisfies

$$\phi_{2,yy}^\perp-\phi_2^\perp+2w\phi_2^\perp-2\frac{\int w\phi_2^\perp\,dy}{\int w^2}w^2=\frac{d}{dy}f_1(y)+g_1(y). \tag{6.15}$$

Note that $\phi_\epsilon^\perp$ cancels the even terms on the r.h.s. Therefore, in the next step, we only have to deal with odd terms.

Step 2.

We multiply (6.12) by $w_y\chi$ and integrate, using the fact that $\int\phi_\epsilon^\perp w_y\chi\,dy=0$. This implies

$$\int L\left[\left(w_y+\epsilon w^0_{1,y}+\epsilon^2 w^0_{2,y}+\epsilon w^0_{3,y}+\epsilon^2 w^0_{4,y}\right)w_y\chi\,dy+\int L[\phi_\epsilon^\perp]w_y\chi\,dy\right]$$
$$=\lambda_\epsilon\int w_y^2\chi\,dy+O(\epsilon|\lambda_\epsilon|). \tag{6.16}$$

Using (6.10) and (6.13), we get

$$\text{r.h.s.}=\lambda_\epsilon\int w_y^2\,dy=1.2\lambda_\epsilon,$$

$$\text{l.h.s.}=-\frac{\epsilon^2}{\xi_0^3}\left(\alpha<\nabla\tilde G(x_1^0,x_1^0)>+<\nabla^2\tilde G(x_1^0,x_1^0)>+<\nabla\nabla\tilde G(x_1^0,x_1^0)>\right)\int yw^2w_y\,dy+\int_{\Omega_\epsilon}w_yL\phi_\epsilon^\perp\,dy$$
$$=\frac{\epsilon^2}{\xi_0^3}\left(\alpha<\nabla\tilde G(x_1^0,x_1^0)>+<\nabla^2\tilde G(x_1^0,x_1^0)>+<\nabla\nabla\tilde G(x_1^0,x_1^0)>\right)\frac{1}{3}\int w^3\,dy+\int_{\Omega_\epsilon}w_yL\phi_\epsilon^\perp\,dy.$$

It remains to estimate $\int_{\Omega_\epsilon}w_yL\phi_\epsilon^\perp\,dy$. We will show that $\int_{\Omega_\epsilon}w_yL\phi_\epsilon^\perp\,dy=O(\epsilon^3)$.

Integration by parts gives

$$\int_{\Omega_\epsilon)} (L_0\phi_\epsilon^\perp) w_y \chi\, dy = \int_{\mathbb{R}} (L_0\phi_\epsilon^\perp) w_y\, dy - 2\frac{\int w\phi_\epsilon^\perp}{\int w^2} \int_{\mathbb{R}} w^2 w_y\, dy + O(\epsilon^3)$$

$$= \int_{\mathbb{R}} L_0[w_y]\phi_\epsilon^\perp\, dy - 2\frac{\int w\phi_\epsilon^\perp}{\int w^2} \int_{\mathbb{R}} w^2 w_y\, dy + O(\epsilon^3) = O(\epsilon^3)$$

since w_y belongs to the kernel of L_0, where $L_0\phi = \phi_{yy} - \phi + 2w\phi$.

Finally, we estimate in the integral if $L\phi_\epsilon^\perp$ is replaced by $L_0\phi_\epsilon^\perp - 2\frac{\int w\phi_\epsilon^\perp}{\int w^2} w^2$:

$$\left| \int_{\Omega_\epsilon} (L\phi_\epsilon^\perp - L_0\phi_\epsilon^\perp + 2\frac{\int w\phi_\epsilon^\perp}{\int w^2} w^2) w_y \chi\, dy \right|$$

$$\le C(\|a_\epsilon - \xi_\epsilon w\|_{H^2(\Omega_\epsilon)}) \|\phi_\epsilon^\perp - \epsilon\phi_1^\perp - \epsilon^2\phi_2^\perp\|_{H^2(\Omega_\epsilon)} = O(\epsilon)(O(\epsilon^3) + O(|\lambda_\epsilon|)) = O(\epsilon^4 + \epsilon|\lambda_\epsilon|).$$

This implies the estimate

$$\int L[\phi_\epsilon^\perp] w_y\, dy = O(\epsilon^4 + \epsilon|\lambda_\epsilon|)$$

for the second term on the r.h.s..

Putting all contributions together, we get

$$\lambda_\epsilon = \frac{\epsilon^2}{1.2\xi_0^3} \left(\alpha < \nabla\tilde{G}(x_1^0, x_1^0) > + < \nabla^2\tilde{G}(x_1^0, x_1^0) > + < \nabla\nabla\tilde{G}(x_1^0, x_1^0) > \right) \frac{1}{3} \int w^3\, dy + O(\epsilon^3)$$

$$= \frac{2\epsilon^2}{\xi_0^3} \left(\alpha < \nabla\tilde{G}(x_1^0, x_1^0) > + < \nabla^2\tilde{G}(x_1^0, x_1^0) > + < \nabla\nabla\tilde{G}(x_1^0, x_1^0) > \right) + O(\epsilon^3).$$

We have stability if

$$\alpha < \nabla\tilde{G}(x_1^0, x_1^0) > + < \nabla^2\tilde{G}(x_1^0, x_1^0) > + < \nabla\nabla\tilde{G}(x_1^0, x_1^0) > < 0.$$

Now we check this condition. Starting with Neumann boundary conditions, we get from (9.39)

$$\lambda_\epsilon = \frac{2\epsilon^2}{\xi_0^3} \left(\alpha < \nabla\tilde{G}(x_1^0, x_1^0) > + < \nabla^2\tilde{G}(x_1^0, x_1^0) > + < \nabla\nabla\tilde{G}(x_1^0, x_1^0) > \right) + O(\epsilon^3)$$

$$= -\frac{\epsilon^2}{D\xi_0^3} \cosh\alpha\, e^{\alpha x_1^0} + O(\epsilon^3)$$

$$= -\frac{\epsilon^2}{D\xi_0^3} \frac{1 + \sqrt{1 + 24Dc\alpha^3 \coth\alpha}}{2\cosh\alpha} + O(\epsilon^3) < 0.$$

For Robin boundary conditions, we compute, using (9.28)

$$\lambda_\epsilon = \frac{2\epsilon^2}{\xi_0^3} \left(\alpha < \nabla\tilde{G}(x_1^0, x_1^0) > + < \nabla^2\tilde{G}(x_1^0, x_1^0) > + < \nabla\nabla\tilde{G}(x_1^0, x_1^0) > \right) + O(\epsilon^3)$$

$$= -\frac{\epsilon^2}{\xi_0^3} \left(\frac{1}{D} + 12c\alpha^2 \right) + O(\epsilon^3) < 0.$$

Theorem 6.1. *The spiky steady states given in Theorem 2.1 and Theorem 2 are both linearly stable. The linearized operator has a small eigenvalue of order $\lambda_\epsilon = O(\epsilon^2)$ as $\epsilon \to 0$.*

For Neumann boundary conditions we have

$$\lambda_\epsilon = -\frac{\epsilon^2}{D\xi_0^3} \frac{1 + \sqrt{1 + 24Dc\alpha^3 \coth\alpha}}{2\cosh\alpha} + O(\epsilon^3) < 0.$$

For Robin boundary conditions we get

$$\lambda_\epsilon = -\frac{\epsilon^2}{\xi_0^3}\left(\frac{1}{D} + 12c\alpha^2\right) + O(\epsilon^3) < 0.$$

Remark: For Neumann boundary conditions the small eigenvalue satisfies

$$\lambda_\epsilon = -\frac{\epsilon^2}{\xi_0^3}\left(\frac{1}{D} + 6c\alpha^2 + O(\alpha^4)\right) + O(\epsilon^3).$$

7. Numerical computations

We conclude this paper confirming our results by numerical computations.
First we consider Neumann boundary conditions for $D = 10$.

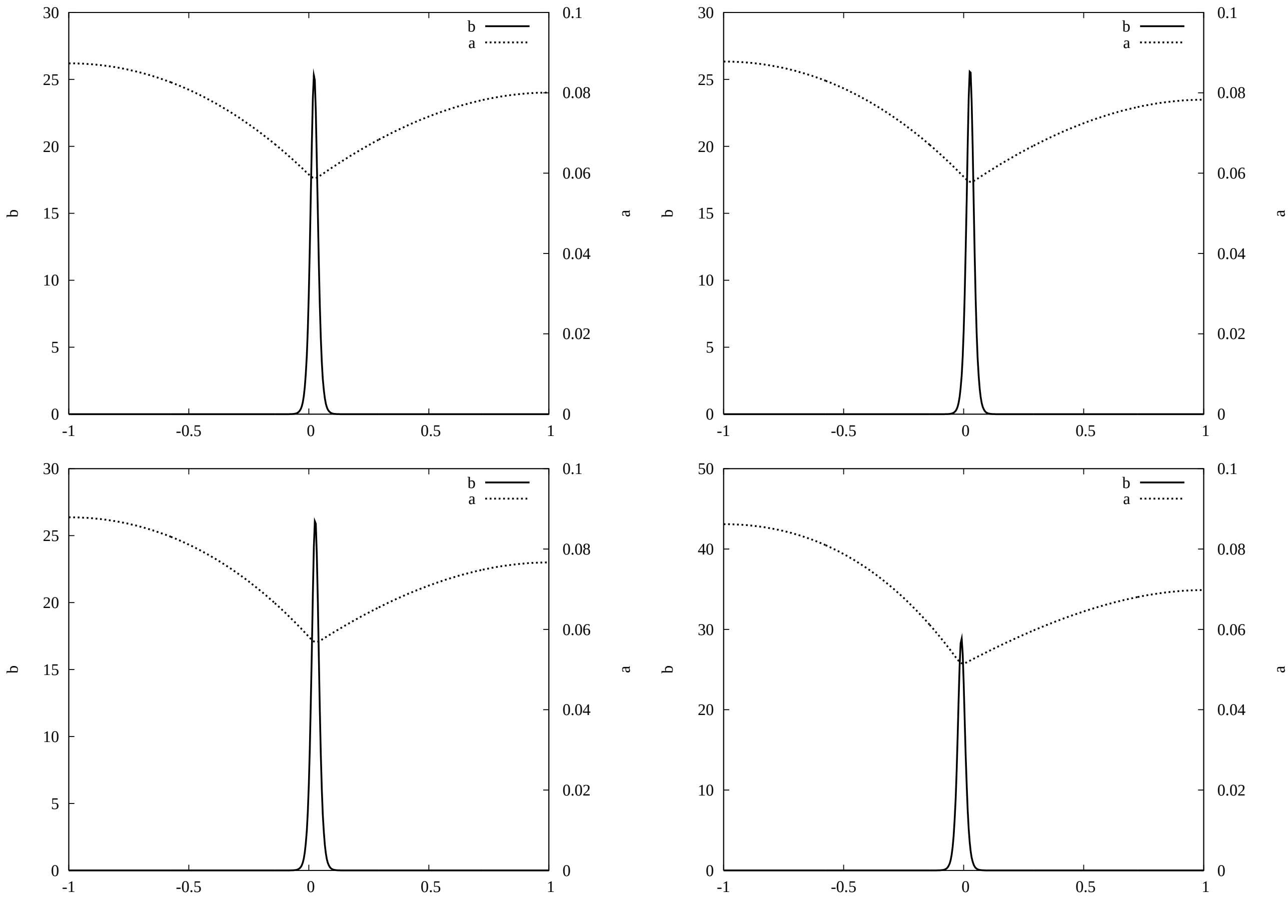

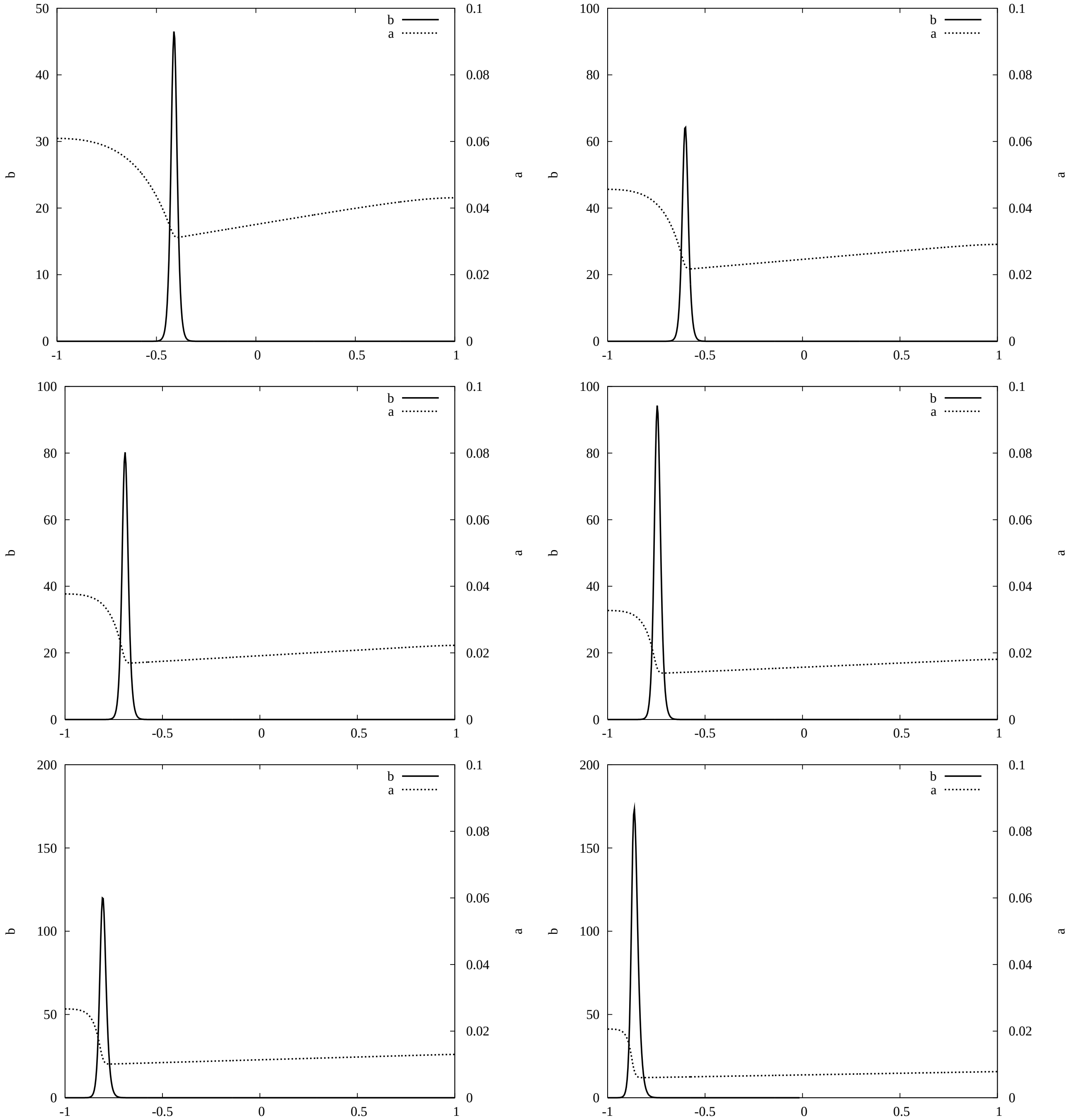
b
a
-1
-0.5
0
0.5
1
0.1
0.08
0.06
0.04
0.02
50
100
150
200

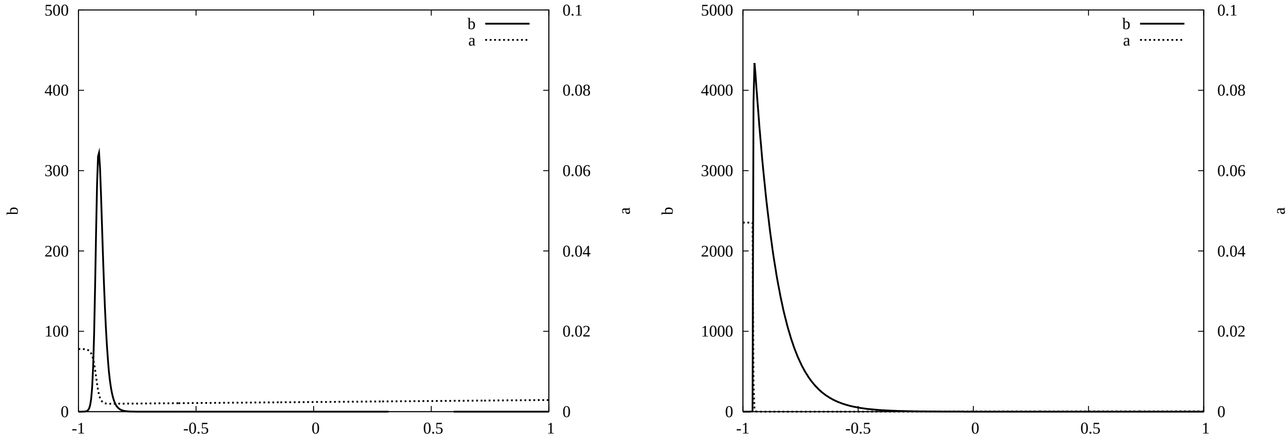

Figure 1. Computation of a spiky steady state for **Neumann boundary conditions** with $\alpha = 0.30$, 0.40, 0.50, 1.0, 5.0, 10, 15, 20, 30, 50, 100, 1000. Starting from the centre position, the spike first moves to the right, then it changes direction and moves to the left and finally approaches the left end of the interval. The other parameters are kept fixed and chosen as $\epsilon = 0.01$, $D = 10$, $c = 0.01$.

Second we consider Neumann boundary conditions again, but now we choose a higher value value of the diffusion constant $D = 50$. We will see that the spike now moves even further to the right than observed in Figure 1 before it turns and moves to the left, finally approaching the left boundary.

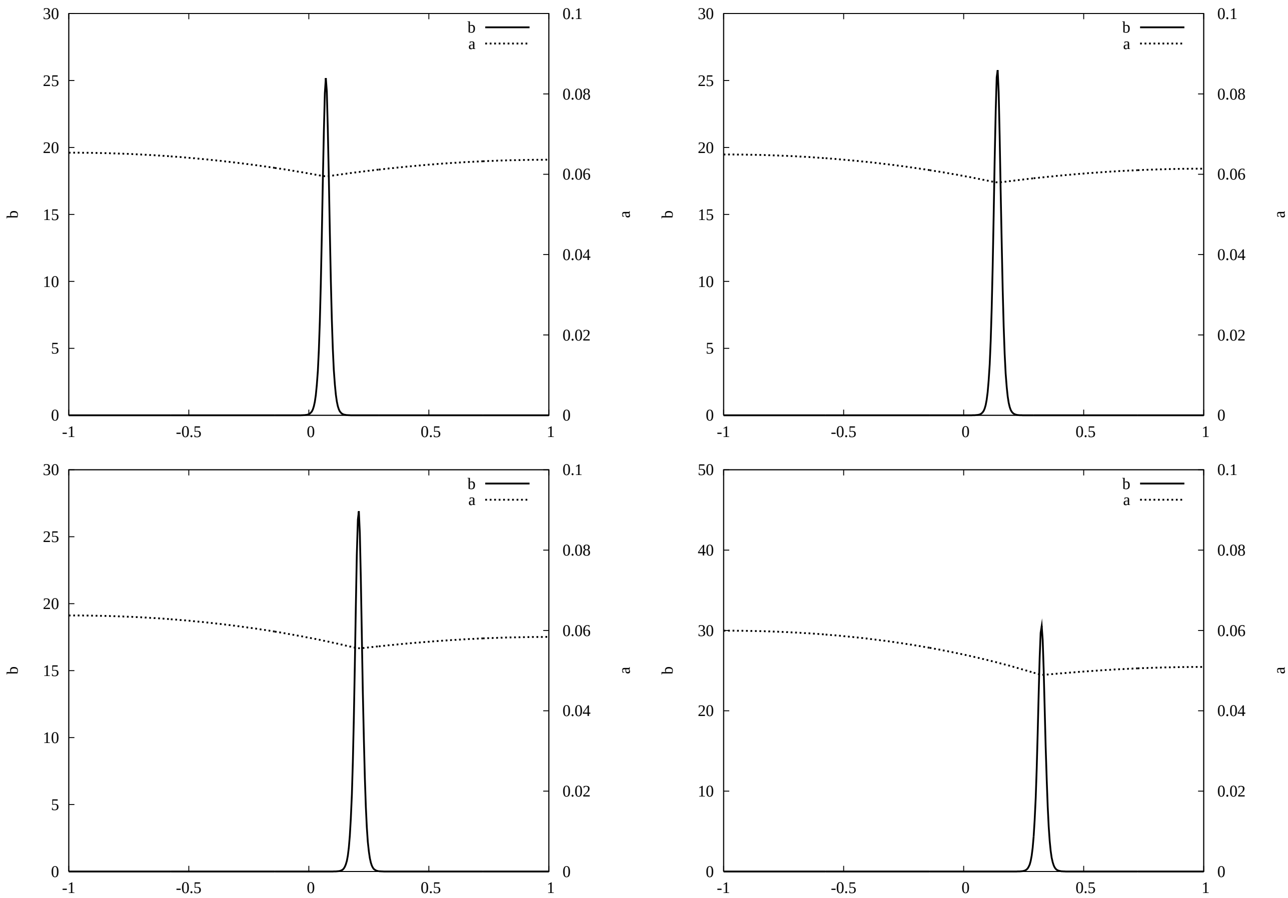

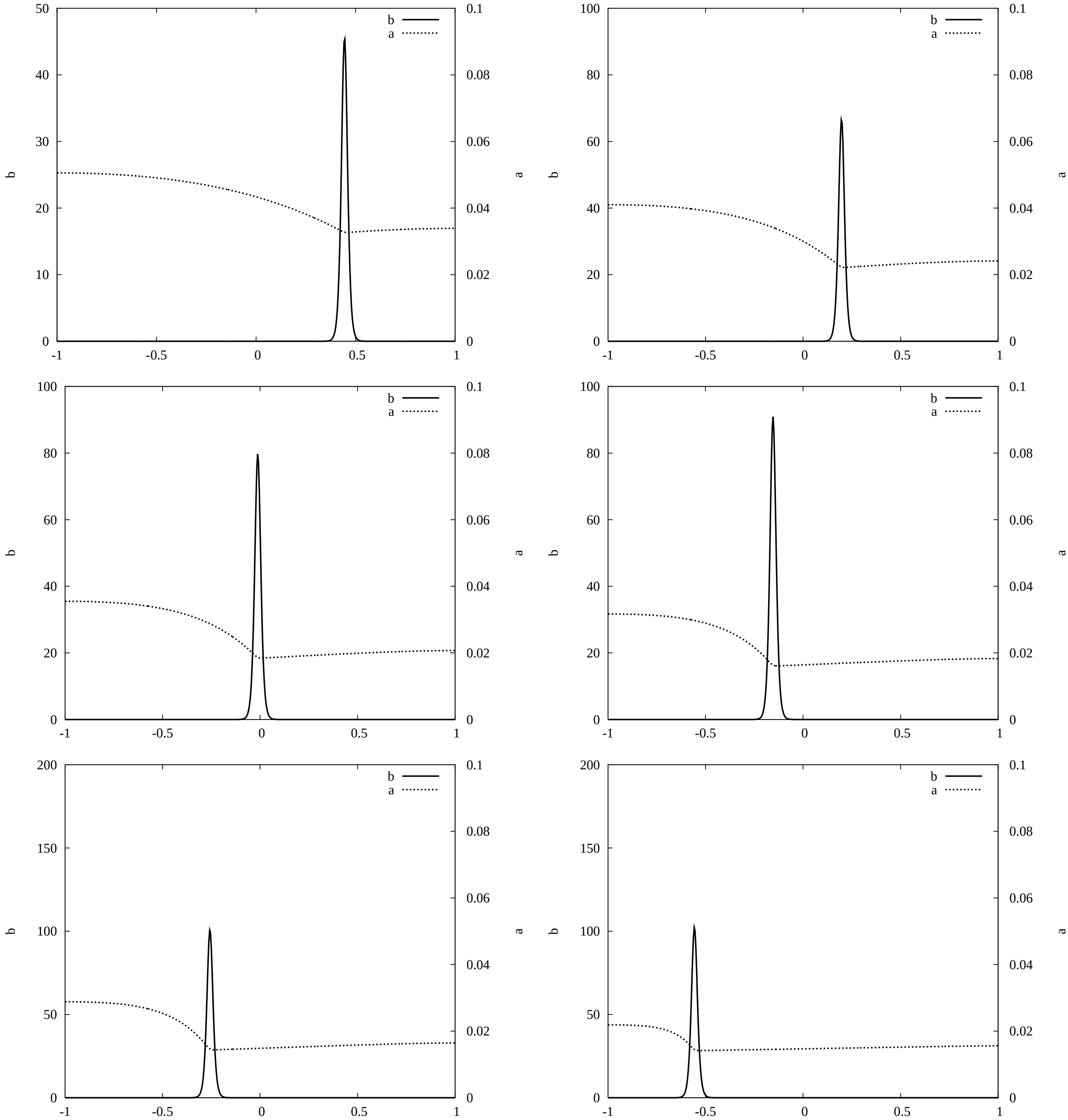
b
a
b
a
b
a
b
a
b
a
b
a

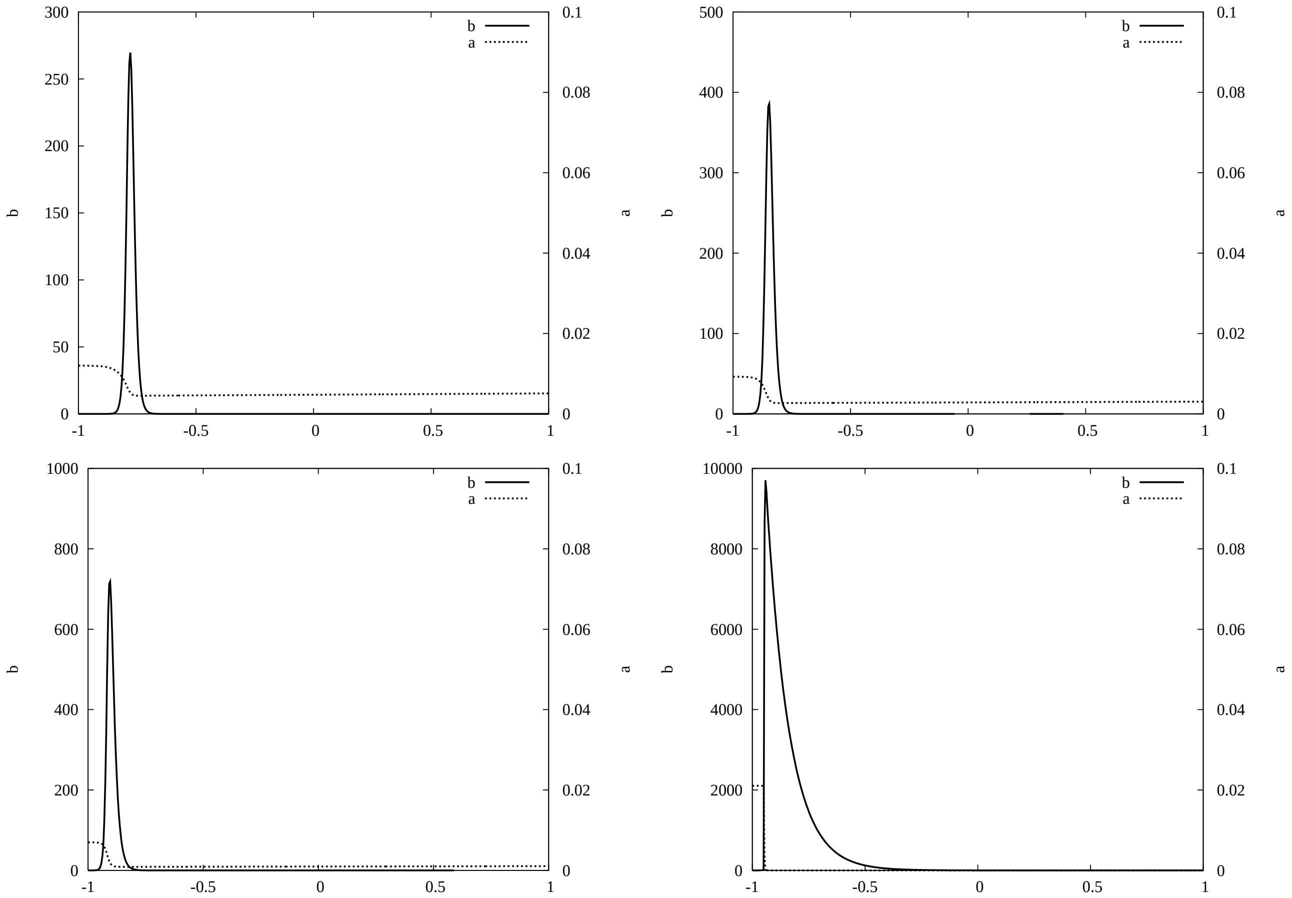

Figure 2. Computation of a spiky steady state for **Neumann boundary conditions** with $\alpha = 0.10, 0.20, 0.30, 0.50, 1.0, 2.0, 3.0, 4.0, 5.0, 10, 30, 50, 100, 1000$. The position of the spike first moves to the right, then it changes direction and moves to the left. Now it moves further to the right than for $D = 10$ (cp. Figure 1). The other constants are chosen as $\epsilon = 0.01$, $D = 50$, $c = 0.01$.

Third we show some computations with Robin boundary conditions. In contrast to the case of Neumann boundary conditions the spike always moves to the right only and does not change direction.

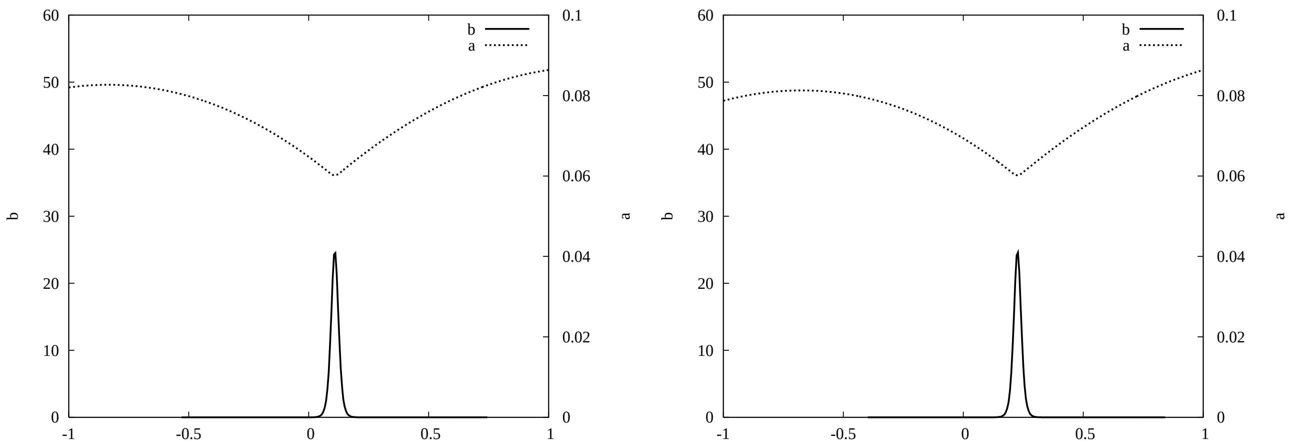

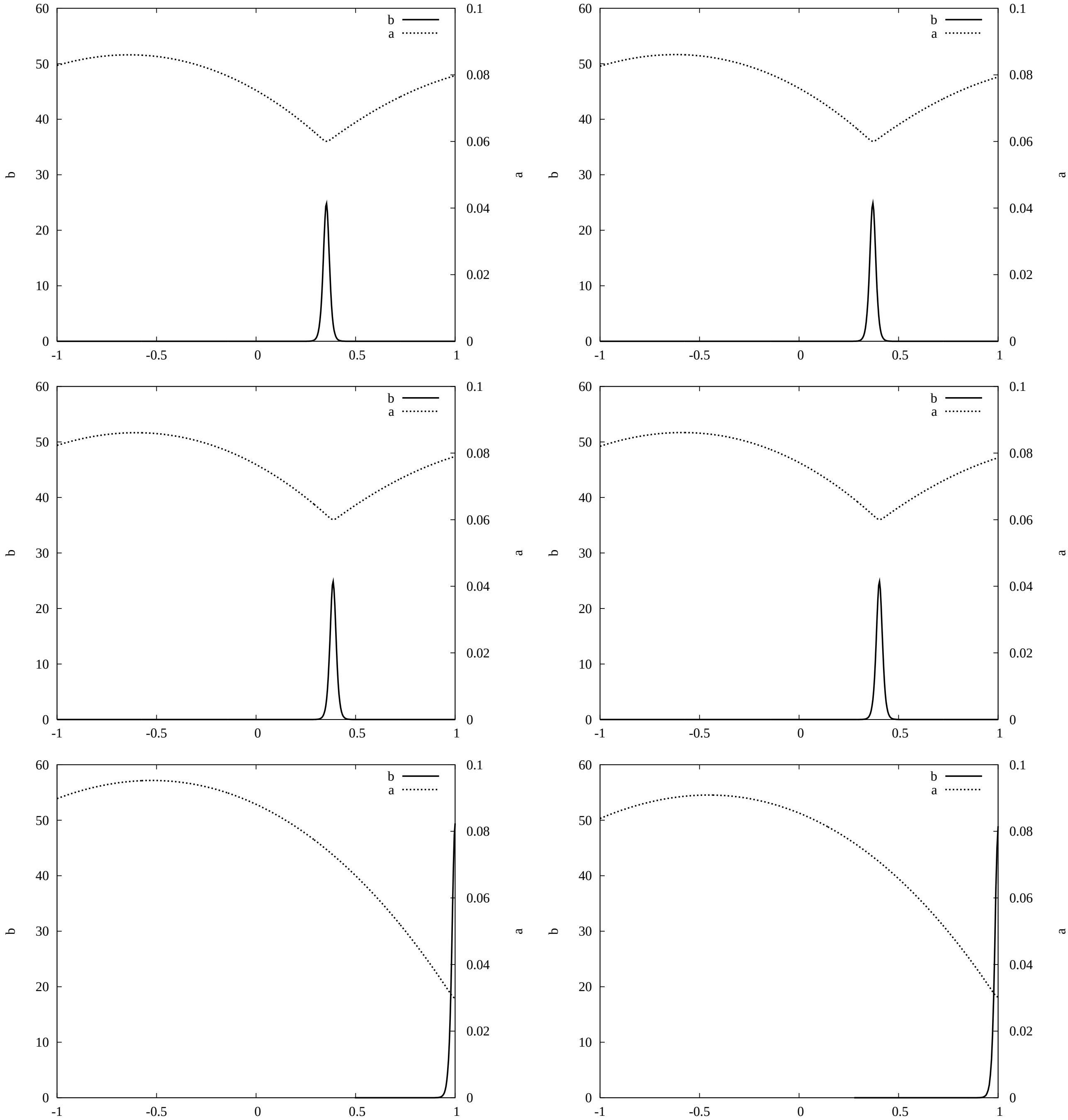

Figure 3. Computation of a spiky steady state for **Robin boundary conditions** with $\alpha = 0.10$, 0.20, 0.21, 0.22, 0.23, 0.24, 0.25, 0.30. The position of the spike moves to the right quickly after α exceeds 0.20. The other constants are chosen as $\epsilon = 0.01$, $D = 10$, $c = 0.01$.

Now we decrease the diffusion constant D. First we consider Neumann boundary conditions. We observe that starting from a single spike we get more and more spikes as D decreases. These multiple spikes have different amplitudes.

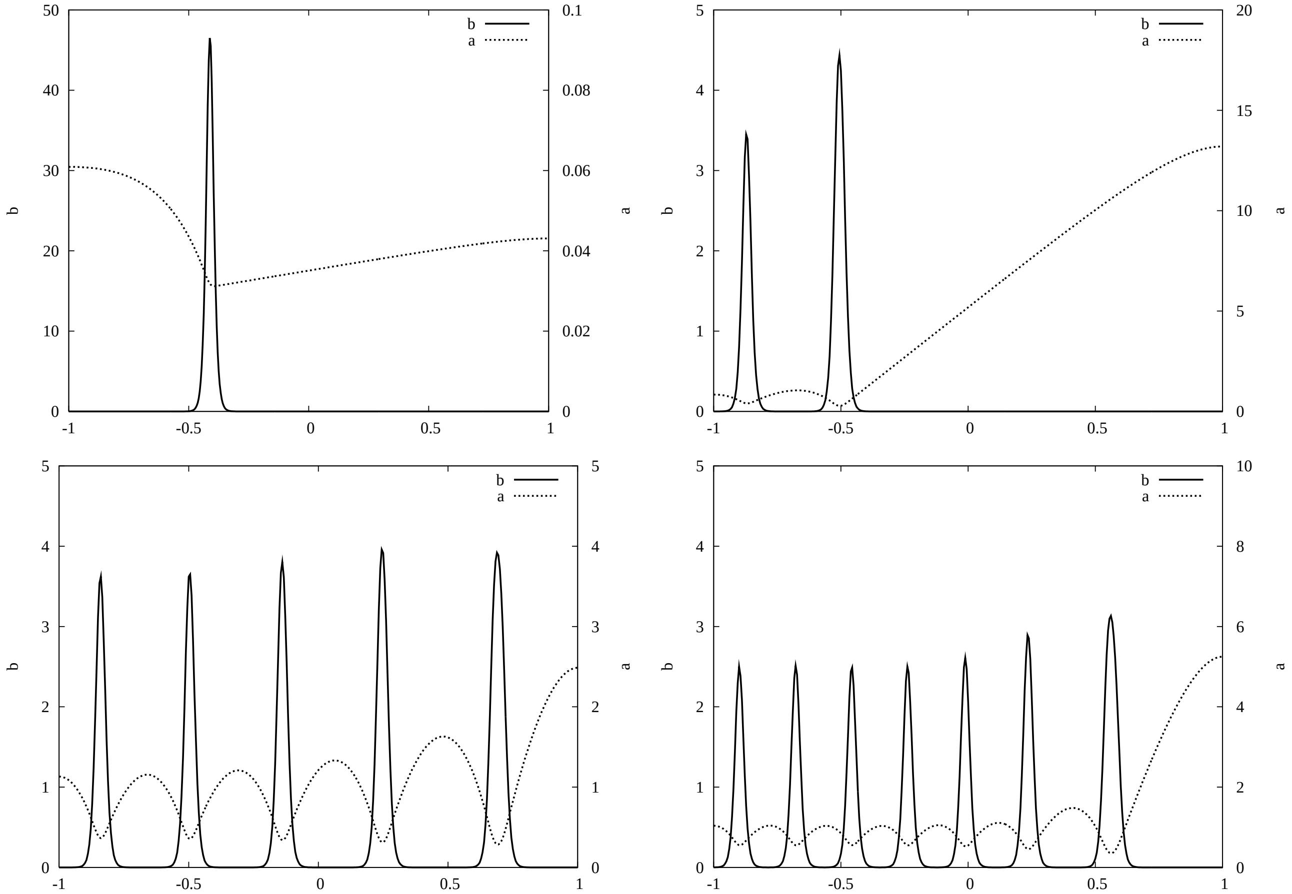

Figure 4. Computation of a steady state with **multiple spikes** for **Neumann boundary conditions** with $\alpha = 5$ and $D = 0.01, 0.008, 0.005$. We observe 2, 5 and 7 spikes, respectively. Note that these multiple spikes have different amplitudes. The other constants are chosen as $\epsilon = 0.01$, $c = 0.01$. For comparison, in the first picture, we plot the solution with a single spike for $D = 10$ again.

Next we compute multiple spikes for Robin boundary conditions. We observe that, starting from a single spike, we get more and more spikes as D decreases. These multiple spikes have different amplitudes.

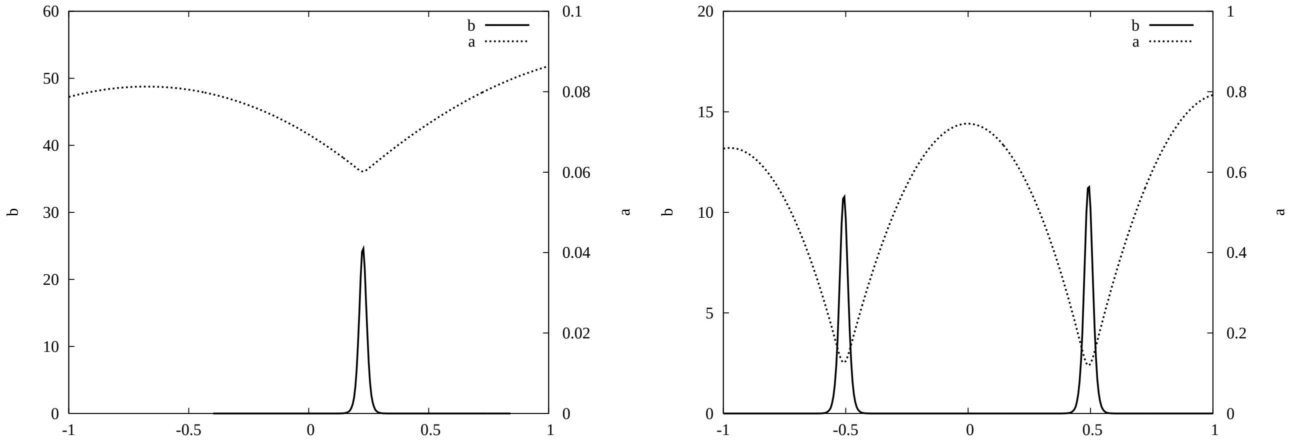

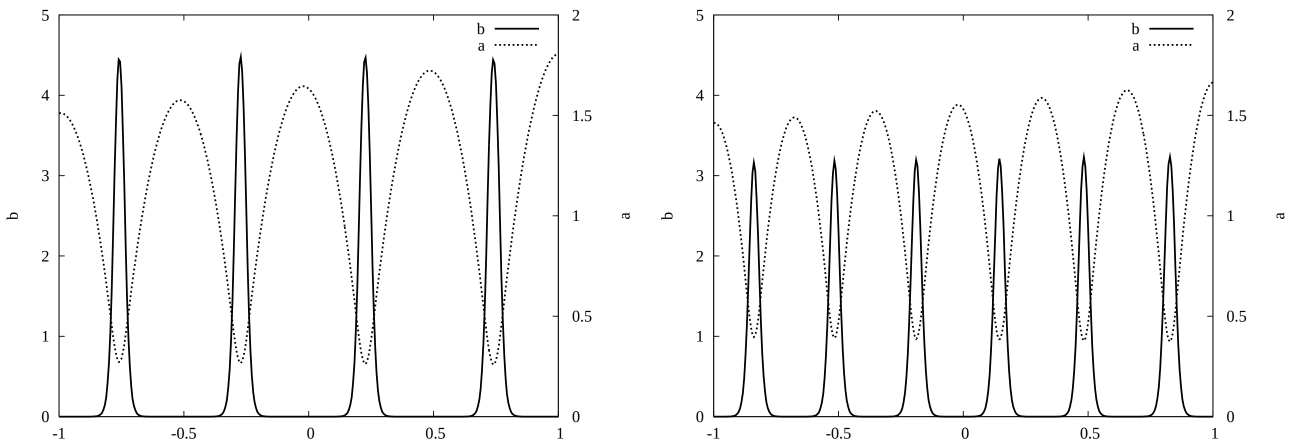

Figure 5. Computation of a steady state with **multiple spikes** for **Robin boundary conditions** with $\alpha = 0.20$ and $D = 0.1, 0.01, 0.005$. We observe 2, 4 and 6 spikes, respectively. Note that these multiple spikes have different amplitudes. The other constants are chosen as $\epsilon = 0.01$, $c = 0.01$. For comparison, in the first graph, we plot again the solution with a single spike for $D = 10$.

To enable an easy comparison between boundary conditions we compute the multiple spikes for Robin boundary conditions again, but now with the same parameters as chosen for Neumann boundary conditions in Figure 4. Note that now the starting configuration shown in the first graph is a boundary spike (in contrast to an interior spike in Figures 4 and 5).

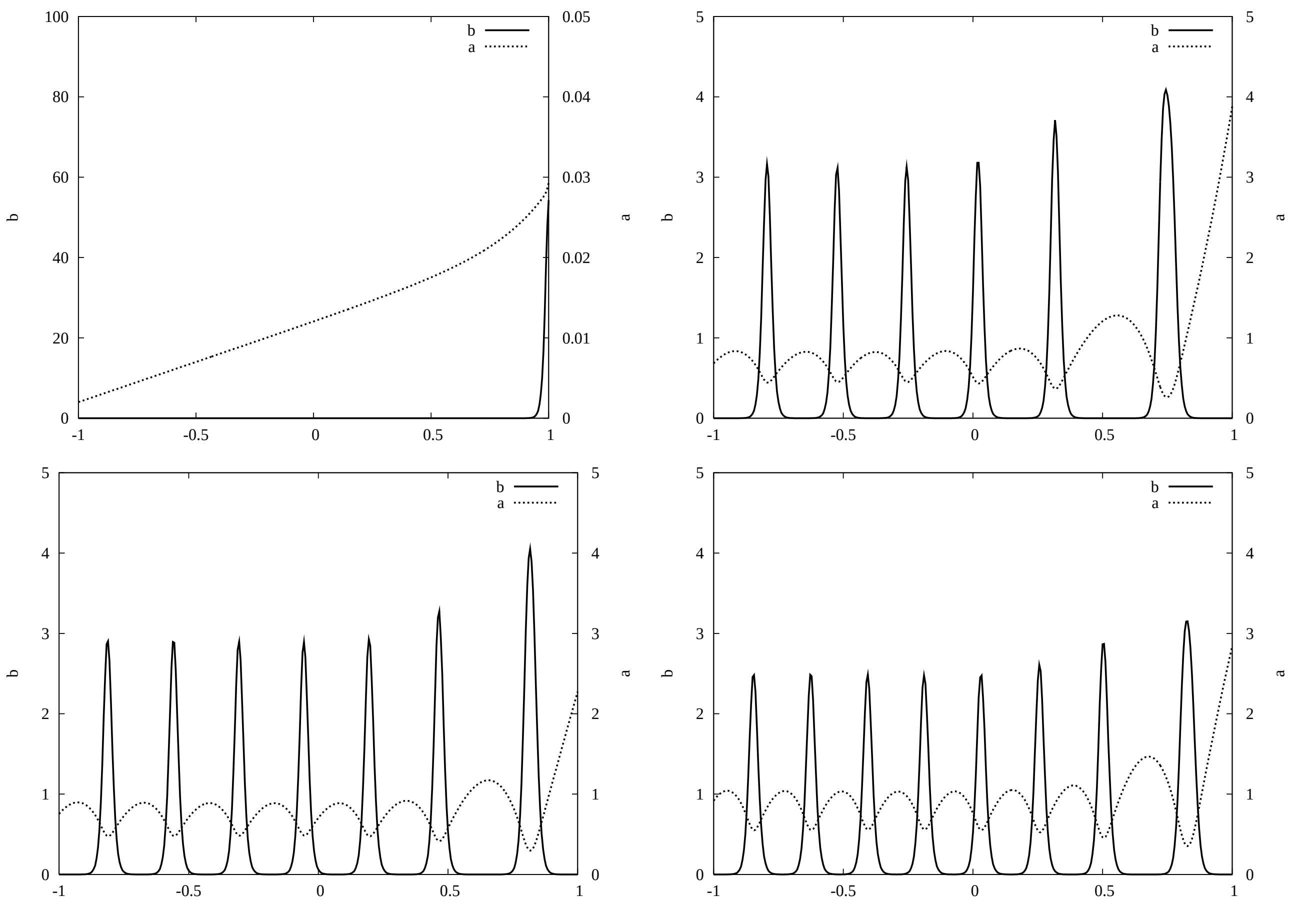

Figure 6. Computation of a steady state with **multiple spikes** for **Neumann boundary conditions** with $\alpha = 5$ and $D = 0.01, 0.008, 0.005$. We observe 6, 7 and 8 spikes, respectively. Note that the spikes have different amplitudes. The other constants are chosen as $\epsilon = 0.01$, $c = 0.01$.

8. Discussion

A very important potential implication of these theoretical results is in the field of symmetry breaking leading to left-right asymmetry. One of the hypotheses tested in recent work in mouse is the effect of a nodal fluid flow leading to the one-sided accumulation of several molecular species mediated by cilia. These models have been reviewed in [5, 13].

The results in this paper capture the interaction of pattern formation by a reaction-diffusion mechanism with convective fluid flow in a simple model problem. In particular, they quantify the effect of asymmetry caused by the flow: The spike is moved from the symmetric position in the centre of the interval to either the left or the right side. The direction of this shift depends on the size of the fluid flow as well as the boundary conditions.

In the biological application of nodal fluid flow in mouse these mathematical results imply that the issue of left-right versus right-left orientation can be affected by various factors such as the size of the flow and the interaction of the pattern-forming system with boundaries such as the cell domain wall.

We show that the shifted spike is stable. In particular, this implies that the new position of the spike is stable and the method of shifting spikes off the center by a convective flow is reliable and reproducable.

9. Appendix A: Representation formulas

In this appendix, we derive representation formulas for the inhibitor part of the solution.

First, we consider **Neumann boundary conditions:**

Let a be the solution of

$$Da_{xx} - D\alpha a_x + \frac{1}{2} - f = 0, \quad a_x(-1) = a_x(1) = 0, \tag{9.1}$$

where $f \in L^2(-1,1)$. We write (9.1) as

$$D(e^{-\alpha x} a_x)_x + \frac{1}{2} e^{-\alpha x} - f e^{-\alpha x} = 0, \quad a_x(-1) = a_x(1) = 0. \tag{9.2}$$

Fix $x_1 \in (-1,1)$. Let $G(x,x_1)$ be the Green's function given by

$$\begin{cases} DG_{xx}(x,x_1) - D\alpha G_x(x,x_1) + \frac{1}{2} - c_{x_1}\delta_{x_1} = 0, \\ G_x(-1,x_1) = G_x(1,x_1) = 0. \end{cases} \tag{9.3}$$

which is equivalent to

$$\begin{cases} D(e^{-\alpha x} G_x(x,x_1))_x + \frac{1}{2} e^{-\alpha x} - c_{x_1} e^{-\alpha x_1}\delta_{x_1} = 0, \\ G_x(-1,x_1) = G_x(1,x_1) = 0. \end{cases} \tag{9.4}$$

(The constant of integration for $G(x, x_1)$ will be determined by (9.7) below.) We first determine the constant c_{x_1}. From (9.4), we have

$$c_{x_1} e^{-\alpha x_1} = \frac{1}{2} \int_{-1}^{1} e^{-\alpha x}\, dx = \frac{\sinh \alpha}{\alpha}. \tag{9.5}$$

Multiplying (9.2) by G, (9.4) by a and integrating, we get

$$\frac{1}{2} \int_{-1}^{1} e^{-\alpha x} G(x, x_1)\, dx - \int_{-1}^{1} f(x) e^{-\alpha x} G(x, x_1)\, dx = \frac{1}{2} \int_{-1}^{1} e^{-\alpha x} a(x)\, dx - c_{x_1} e^{-\alpha x_1} a(x_1).$$

Hence, using (9.5),

$$\frac{\sinh \alpha}{\alpha} a(x_1) = \frac{1}{2} \int_{-1}^{1} e^{-\alpha x} a(x)\, dx - \frac{1}{2} \int_{-1}^{1} e^{-\alpha x} G(x, x_1)\, dx + \int_{-1}^{1} f(x) e^{-\alpha x} G(x, x_1)\, dx. \tag{9.6}$$

Let us choose the constant of integration for the Green's function such that

$$\int_{-1}^{1} e^{-\alpha x} G(x, x_1)\, dx = 0. \tag{9.7}$$

Then we have the following representation formula for a:

$$a(x_1) = \frac{\alpha}{2 \sinh \alpha} \int_{-1}^{1} e^{-\alpha x} a(x)\, dx + \frac{\alpha}{\sinh \alpha} \int_{-1}^{1} f(x) e^{-\alpha x} G(x, x_1)\, dx. \tag{9.8}$$

Now, if we let

$$f(x) = c_{x_0} \delta_{x_0},$$

we get from (9.1), (9.3)

$$a(x) = G(x, x_0)$$

and so (9.8) implies

$$G(x_1, x_0) = \frac{\alpha}{2 \sinh \alpha} \int_{-1}^{1} e^{-\alpha x} G(x, x_0)\, dx + \frac{\alpha}{\sinh \alpha} e^{-\alpha x_0} G(x_0, x_1).$$

Using (9.7), we get

$$G(x_1, x_0) = \frac{\alpha}{\sinh \alpha} e^{-\alpha x_0} G(x_0, x_1).$$

Now (9.5) implies that

$$G(x_1, x_0) = G(x_0, x_1). \tag{9.9}$$

For later use, we compute the Green's function explicitly. Using the boundary conditions, continuity and jump condition at x_1, we get

$$G(x, z) = \begin{cases} \frac{1}{2D\alpha}(x + z) - \frac{1}{2D\alpha^2}(e^{\alpha(x+1)} + e^{\alpha(z-1)}) + c, & -1 < x < z, \\ \frac{1}{2D\alpha}(x + z) - \frac{1}{2D\alpha^2}(e^{\alpha(x-1)} + e^{\alpha(z+1)}) + c, & z < x < 1. \end{cases}$$

We compute the constant c, using (9.7), which gives $c = \frac{1}{D\alpha} \coth \alpha$. Finally, we get

$$G(x, z) = \begin{cases} \frac{1}{2D\alpha}(x + z) - \frac{1}{2D\alpha^2}(e^{\alpha(x+1)} + e^{\alpha(z-1)}) + \frac{1}{D\alpha} \coth \alpha, & -1 < x < z, \\ \frac{1}{2D\alpha}(x + z) - \frac{1}{2D\alpha^2}(e^{\alpha(x-1)} + e^{\alpha(z+1)}) + \frac{1}{D\alpha} \coth \alpha, & z < x < 1. \end{cases} \tag{9.10}$$

Second, we consider **Robin boundary conditions:**

Let a be the solution of

$$D a_{xx} - D\alpha a_x + \frac{1}{2} - f = 0, \quad a_x(-1) - \alpha a(-1) = a_x(1) - \alpha a(1) = 0, \tag{9.11}$$

where $f \in L^2(-1,1)$. We write (9.11) as

$$D(e^{-\alpha x}a_x)_x + \frac{1}{2}e^{-\alpha x} - fe^{-\alpha x} = 0, \quad a_x(-1) - \alpha a(-1) = a_x(1) - \alpha a(1) = 0. \tag{9.12}$$

Fix $x_1 \in (-1,1)$. Let $G(x, x_1)$ be the Green's function given by

$$\begin{cases} DG_{xx}(x,x_1) - D\alpha G_x(x,x_1) + \frac{1}{2} - c_{x_1}\delta_{x_1} = 0, \\ G_x(-1,x_1) - \alpha G(-1,x_1) = G_x(1,x_1) - \alpha G(1,x_1) = 0. \end{cases} \tag{9.13}$$

which is equivalent to

$$\begin{cases} D(e^{-\alpha x}G_x(x,x_1))_x + \frac{1}{2}e^{-\alpha x} - c_{x_1}e^{-\alpha x_1}\delta_{x_1} = 0, \\ G_x(-1,x_1) - \alpha G(-1,x_1) = G_x(1,x_1) - \alpha G(1,x_1) = 0. \end{cases} \tag{9.14}$$

(The constant of integration will be fixed by (9.7).) We first determine c_{x_1}. From (9.13), we have

$$c_{x_1} = 1. \tag{9.15}$$

Multiplying (9.12) by G, (9.14) by a and integrating, we get

$$\frac{1}{2}\int_{-1}^{1} e^{-\alpha x}G(x,x_1)\,dx - \int_{-1}^{1} f(x)e^{-\alpha x}G(x,x_1)\,dx = \frac{1}{2}\int_{-1}^{1} e^{-\alpha x}a(x)\,dx - e^{-\alpha x_1}a(x_1).$$

Hence, using (9.7) and (9.15), we get the following representation formula for a:

$$a(x_1) = \frac{1}{2}e^{\alpha x_1}\int_{-1}^{1} e^{-\alpha x}a(x)\,dx + e^{\alpha x_1}\int_{-1}^{1} f(x)e^{-\alpha x}G(x,x_1)\,dx. \tag{9.16}$$

Now, if we let

$$f(x) = c_{x_0}\delta_{x_0},$$

we get (9.11), (9.13)

$$a(x) = G(x, x_0)$$

and so (9.16) implies

$$G(x_1,x_0) = \frac{1}{2}e^{\alpha x_1}\int_{-1}^{1} e^{-\alpha x}G(x,x_0)\,dx + e^{\alpha x_1}e^{-\alpha x_0}G(x_0,x_1).$$

Using (9.7), we get the symmetry relation

$$e^{-\alpha x_1}G(x_1,x_0) = e^{-\alpha x_0}G(x_0,x_1). \tag{9.17}$$

For later use, we compute the Green's function explicitly. Using the boundary conditions, continuity and jump condition at x_1, we get

$$e^{-\alpha x}G(x,z) = \begin{cases} \left(\frac{x}{2D\alpha} + \frac{1}{2D\alpha^2} + \frac{1}{2D\alpha}\right)e^{-\alpha x} + \left(\frac{z}{2D\alpha} + \frac{1}{2D\alpha^2} - \frac{1}{2D\alpha}\right)e^{-\alpha z} + c, & -1 < x < z, \\ \left(\frac{x}{2D\alpha} + \frac{1}{2D\alpha^2} - \frac{1}{2D\alpha}\right)e^{-\alpha x} + \left(\frac{z}{2D\alpha} + \frac{1}{2D\alpha^2} + \frac{1}{2D\alpha}\right)e^{-\alpha z} + c, & z < x < 1. \end{cases}$$

We compute the constant c, using (9.7), which gives $c = -\frac{\sinh\alpha}{2D\alpha^3}$. Finally, we get

$$G(x,z) = \begin{cases} \left(\frac{x}{2D\alpha} + \frac{1}{2D\alpha^2} + \frac{1}{2D\alpha}\right) + \left(\frac{z}{2D\alpha} + \frac{1}{2D\alpha^2} - \frac{1}{2D\alpha}\right)e^{\alpha(x-z)} - \frac{\sinh\alpha}{2D\alpha^3}e^{\alpha x}, & -1 < x < z, \\ \left(\frac{x}{2D\alpha} + \frac{1}{2D\alpha^2} - \frac{1}{2D\alpha}\right) + \left(\frac{z}{2D\alpha} + \frac{1}{2D\alpha^2} + \frac{1}{2D\alpha}\right)e^{\alpha(x-z)} - \frac{\sinh\alpha}{2D\alpha^3}e^{\alpha x}, & z < x < 1. \end{cases} \tag{9.18}$$

For later use we make the following computations for **Robin boundary conditions**. First, we recall from (3.7) that

$$a(z) = \frac{1}{2}e^{\alpha z}\int_{-1}^{1} e^{-\alpha x}a(x)\,dx + (e^{\alpha(z-x)}G(x,z))|_{x=P} + O(\epsilon). \tag{9.19}$$

Setting $z = P$, we get

$$\frac{1}{2}\int_{-1}^{1} e^{-\alpha x}a(x)\,dx = e^{-\alpha P}(6c - G(x,P)) + O(\epsilon). \tag{9.20}$$

Substituting (9.20) into (9.19), we get

$$a(z) = e^{\alpha(z-P)}6c + e^{\alpha(z-x)}(G(x,z) - G(x,P)) + O(\epsilon) = \tilde{G}(x,z) + O(\epsilon). \tag{9.21}$$

We recall from (3.11) that

$$\tilde{G}(x,z) = e^{\alpha(z-P)}6c + e^{\alpha(z-x)}(G(x,z) - G(x,P)).$$

Taking the first derivative w.r.t. z in (9.21) and setting $z = P$, we get

$$a'(P) = 6\alpha c + < \nabla_z G(P,P) > + O(\epsilon) = < \nabla_z \tilde{G}(P,P) > + O(\epsilon). \tag{9.22}$$

Taking the second derivative w.r.t. z, we get for $z = P$

$$a''(P) = 6\alpha^2 c + 2\alpha < \nabla_z G(P,P) > + < \nabla_z^2 G(P,P) > + O(\epsilon) = < \nabla_z^2 \tilde{G}(P,P) > + O(\epsilon), \tag{9.23}$$

using (9.22). Similarly to (9.19), we derive

$$\psi(z) = \frac{1}{2}e^{\alpha z}\int_{-1}^{1} e^{-\alpha x}\psi(x)\,dx - \nabla_x < e^{\alpha(z-x)}G(x,z) > |_{x=P} + O(\epsilon). \tag{9.24}$$

Integrating the equation for ψ given in (4.2), we get for $\psi(P) + O(\epsilon)$. This implies, together with (9.24) with $z = P$,

$$\frac{1}{2}e^{\alpha P}\int_{-1}^{1} e^{-\alpha x}\psi(x)\,dx = < \nabla_x(e^{\alpha(P-x)}G(P,P)) > + O(\epsilon). \tag{9.25}$$

and so

$$\psi(z) = e^{\alpha(z-P)} < \nabla_x(e^{\alpha(P-x)}G(P,P)) > - < \nabla_x(e^{\alpha(z-x)}G(x,z)) > |_{x=P} + O(\epsilon) \tag{9.26}$$

Taking a derivative w.r.t. z in (9.24), we get

$$\begin{aligned}\psi'(z) &= \nabla_z e^{\alpha(z-P)} < \nabla_x(e^{\alpha(P-x)}G(x,P) > - < \nabla_x\nabla_z(e^{\alpha(z-x)}G(x,z)) > + O(\epsilon)\\ &= < \nabla_x\nabla_z(e^{\alpha(z-x)}(G(x,P) - G(x,z)) > + O(\epsilon)\\ &= - < \nabla_x\nabla_z\tilde{G}(x,z) > + O(\epsilon).\end{aligned} \tag{9.27}$$

Using (9.18), we compute

$$\tilde{G}(x,z) = 6ce^{\alpha(z-P)} + \left(\frac{z}{2D\alpha} + \frac{1}{2D\alpha^2} \mp \frac{1}{2D\alpha}\right) - \left(\frac{P}{2D\alpha} + \frac{1}{2D\alpha^2} \mp \frac{1}{2D\alpha}\right)e^{\alpha(z-P)},$$

where the upper or lower sign applies for $-1 < x < z$ and $z < x < 1$, respectively. This implies

$$< \nabla_z\tilde{G}(x,z) > = 6c\alpha - \frac{P}{2D} + O(\epsilon),$$

$$< \nabla_z^2 \tilde{G}(x,z) >= 6c\alpha^2 - \frac{P\alpha}{2D} - \frac{1}{2D} + O(\epsilon),$$
$$< \nabla_x \nabla_z \tilde{G}(x,z) >= O(\epsilon)$$

which implies, using (3.5),

$$\alpha < \nabla_z \tilde{G}(x,z) > + < \nabla_z^2 \tilde{G}(x,z) > + < \nabla_x \nabla_z \tilde{G}(x,z) >$$
$$= 12c\alpha^2 - \frac{P\alpha}{D} - \frac{1}{2D} + O(\epsilon) = -6c\alpha^2 - \frac{1}{2D} + O(\epsilon). \tag{9.28}$$

Similarly, for **Neumann boundary conditions**, we compute the following:

First, we recall from (2.11) that

$$a(z) = \frac{\alpha}{2\sinh\alpha} \int_{-1}^{1} e^{-\alpha x} a(x)\, dx + e^{\alpha(P-x)} G(x,z) + O(\epsilon). \tag{9.29}$$

Setting $z = P$, we get

$$\frac{\alpha}{2\sinh\alpha} \int_{-1}^{1} e^{-\alpha x} a(x)\, dx = \frac{\alpha}{\sinh\alpha} 6ce^{-\alpha P} - \tilde{G}(P,P) + O(\epsilon), \tag{9.30}$$

where

$$\tilde{G}(x,z) = e^{\alpha(P-x)} G(x,z).$$

Substituting (9.30) into (9.29), we get

$$a(z) = \frac{\alpha}{\sinh\alpha} 6ce^{-\alpha P} + (\tilde{G}(x,z) - \tilde{G}(x,P)) + O(\epsilon). \tag{9.31}$$

Taking the derivative w.r.t. z in (9.31) and setting $z = P$, we get

$$a'(P) =< \nabla_z \tilde{G}(P,P) > + O(\epsilon). \tag{9.32}$$

Taking a second derivative w.r.t. z, we get

$$a''(P) =< \nabla_z^2 \tilde{G}(P,P) > + O(\epsilon), \tag{9.33}$$

using (9.32). Similarly, we derive

$$\psi(z) = \frac{\alpha}{2\sinh\alpha} \int_{-1}^{1} e^{-\alpha x} \psi(x)\, dx - < \nabla_x \tilde{G}(x,z)|_{x=z} > + O(\epsilon). \tag{9.34}$$

Integrating the equation for ψ given in (4.2), we get

$$\psi(P) = O(\epsilon) = (- < \nabla_x \tilde{G}(P,z) > + < \nabla_x \tilde{G}(P,P) >) + O(\epsilon). \tag{9.35}$$

Setting $z = P$, we get

$$\frac{\alpha}{2\sinh\alpha} \int_{-1}^{1} e^{-\alpha x} \psi(x)\, dx = \nabla_x \tilde{G}(P,P) + O(\epsilon). \tag{9.36}$$

Substituting (9.36) into (9.34), we get

$$\psi(z) = - < \nabla_x \tilde{G}(P,z) > + < \nabla_x \tilde{G}(P,P) > + O(\epsilon). \tag{9.37}$$

Taking a derivative w.r.t. z in (9.37) and setting $z = P$, we get

$$\psi'(z) = - < \nabla_x \nabla_z \tilde{G}(x,z) > + < \nabla_x \nabla_z \tilde{G}(x,P) > + O(\epsilon). \tag{9.38}$$

Using (9.10), we compute

$$\tilde{G}(x,z) = e^{\alpha(P-x)} G(x,z)$$

$$= \frac{1}{2D\alpha}(x+z)e^{\alpha(P-x)} - \frac{1}{2D\alpha^2}\left(e^{\alpha(P\pm1)} + e^{\alpha(z+P-x\mp1)}\right) + \frac{1}{D\alpha}\coth\alpha\, e^{\alpha(P-x)},$$

$$\nabla_z\tilde{G}(P,P) = \frac{1}{2D\alpha}\left(1 - e^{\alpha(P\mp1)}\right),$$

$$< \nabla_z\tilde{G}(P,P) >= \frac{1}{2D\alpha}\left(1 - \cosh\alpha\, e^{\alpha P}\right),$$

$$\nabla_z^2\tilde{G}(P,P) = -\frac{1}{2D}e^{\alpha(P\mp1)}$$

which implies

$$< \nabla_z^2\tilde{G}(P,P) >= -\frac{1}{2D}\cosh\alpha\, e^{\alpha P}.$$

Taking a derivative w.r.t. x, we get

$$\nabla_x\nabla_z\tilde{G}(P,P) = -\frac{1}{2D}\left(1 - e^{\alpha(P\mp1)}\right),$$

$$< \nabla_x\nabla_z G(P,P) >= -\frac{1}{2D}(1 - \cosh\alpha\, e^{\alpha P})$$

which implies, using (2.7),

$$\begin{aligned}\alpha < \nabla_z\tilde{G}(x,z) > + < \nabla_z^2\tilde{G}(x,z) > + < \nabla_x\nabla_z\tilde{G}(x,z) >\\ = -\frac{1}{2D}\cosh\alpha e^{\alpha P} + O(\epsilon)\\ = -\frac{1}{2D}\frac{1+\sqrt{1+24Dc\alpha^3\coth\alpha}}{2\cosh\alpha} + O(\epsilon).\end{aligned} \tag{9.39}$$

Acknowledgments. The research of JW is supported by an Earmarked Grant from RGC of Hong Kong. MW thanks the Department of Mathematics at CUHK for their kind hospitality.

References

[1] P. Andresen, M. Bache, E. Mosekilde, G. Dewel and P. Borckmans, Stationary space-periodic structures with equal diffusion coefficients, *Phys. Rev. E* 60 (1999), 297-301.

[2] N.A. Brown and L. Wolpert, The development of handedness in left/right asymmetry, *Development* 109 (1990), 1-9.

[3] E.N. Dancer, On stability and Hopf bifurcations for chemotaxis systems, *Meth. Appl. Anal.* 8 (2001), 245-256.

[4] D. Gilbarg and N. S. Trudinger, *Elliptic Partial Differential Equations of Second Order,* 2nd edition, Springer, Berlin, 1983.

[5] H. Hamada, C. Meno, D. Watanabe and Y. Saijoh, Establishment of vertebrate left-right asymmetry, *Nat. Rev. Genet.* 3 (2002), 103-113.

[6] J.S. Huxley and G.R. de Beer, The Elements of Experimental Embryology, New York: Heffner.

[7] D. Iron J. Wei and M. Winter, Stability analysis of Turing patterns generated by the Schnakenberg model, *J. Math. Biol.* 49 (2004), 358-390.

[8] M. Kaern and M. Menzinger, Experimental observation of stationary chemical waves in a flow system, *Phys. Rev. E* 60 (1999), 3471-3474.

[9] P. V. Kuptsov, S. P. Kuznetsov and E. Mosekilde, Particle in the Brusselator model with flow, *Phys. D* 163 (2002), 80-88.

[10] S. Kuznetsov, G. Dewel, E. Mosekilde, P. Borckmans, Absolute and convective instabilities in a one-dimensional Brusselator flow model, *J. Chem. Phys.* 106 (1997), 7609-7616.

[11] J. H. Merkin, R. A. Satnoianu and S. K. Scott, The development of spatial structure in an ionic chemical system induced by applied electric fields, *Dyn. Stabil. Syst.* 15 (2000), 209-230.

[12] J. H. Merkin, H. Sevcikova, D. Snita and M. Marek, The effects of an electric fields on an autocatalytic ionic reaction in a system with high ionic strength, *IMA J. Appl. Math.* 60 (1998), 1-31.

[13] A. Raya and J. C. I. Belmonte, Left-right asymmetry in the vertebrate embryo: from early information to higher-level integration, Nat. Rev. Genet. 7 (2006), 283-293.

[14] A. B. Rovinsky and M. Menzinger, Chemical instability induced by a differential flow, *Phys. Rev. Lett.* 69 (1992), 1193-1196.

[15] A. B. Rovinsky and M. Menzinger, Self-organisation induced by the differential flow of activator and inhibitor, *Phys. Rev. Lett.* 70 (1993), 778-781.

[16] R. A. Satnoianu, P. K. Maini and M. Menzinger, Parameter space analysis, pattern sensitivity and model comparison for Turing and stationary flow-distributed waves (FDS), *Phys. D* 160 (2001), 79-102.

[17] R. A. Satnoianu and M. Menzinger, Non-Turing stationary patterns: flow-distributed stationary structures with general diffusion and flow rates, *Phys. Rev. E* 62 (2000), 113-119.

[18] R. A. Satnoianu and M. Menzinger, A general mechanism for "inexact" phase differences in reaction-diffusion-advection systems, *Phys. Lett. A* 304 (2002), 149-156.

[19] R. A. Satnoianu, M. Menzinger and P. K. Maini, Turing instabilities in general systems, *J. Math. Biol.* 41 (2000), 493-512.

[20] R. A. Satnoianu, J. H. Merkin and S. K. Scott, Spatio-temporal structures in a differential flow reactor with cubic autocatalator kinetics, *Phys. D* 124 (1998), 354-367.

[21] R. A. Satnoianu, J. H. Merkin and S. K. Scott, Forced convective structure in a differential-flow reactor with cubic autocatalytics kinetics, *Dyn. Stabil. Syst.* 14 (1999), 275-298.

[22] B. Schmidt, P. De Kepper and S. C. Müller, Destabilization of Turing structures by electric fields, *Phys. Rev. Lett.* 90 (2003), 118302.

[23] J. Wei, On the construction of single-peaked solutions to a singularly perturbed semilinear Dirichlet problem, *J. Differential Equations* 129 (1996), 315-333.

[24] J. Wei, On single interior spike solutions of Gierer-Meinhardt system: uniqueness, spectrum estimates and stability analysis, *Euro. J. Appl. Math.* 10 (1999), 353-378.

[25] J. Wei and M. Winter, Spikes for the two-dimensional Gierer-Meinhardt system: the weak coupling case, *J. Nonlinear Sci.* 11 (2001), 415-458.

[26] J. Wei and M. Winter, Existence and stability analysis of asymmetric patterns for the Gierer-Meinhardt system, *J. Math. Pures Appl.* 83 (2004), 433-476.

[27] J. Wei and M. Winter, Existence, classification and stability analysis of multiple-peaked solutions for the Gierer-Meinhardt system in R^1, *Methods Appl. Anal.* 14 (2007), 119-164.

[28] J. Wei and M. Winter, Stationary multiple spots for reaction-diffusion systems, *J. Math. Biol.* 57 (2008), 53-89.